

# ROBUST FAULT-TOLERANT CONTROL FOR AIRCRAFT SYSTEMS

A Thesis

Submitted to the Graduate Faculty of the  
Louisiana State University and  
Agricultural and Mechanical College  
in partial fulfillment of the  
requirements for the degree of  
Master of Science in Electrical Engineering

in

The Department of Electrical and Computer Engineering

by

Phalguni Kumar Rachinayani  
Bachelor of Technology,  
Jawaharlal Nehru Technological University, May 2002  
August 2006

*To my Mother*  
*R. Jaya Bharathi*

# Acknowledgements

First I would like to thank my adviser and mentor Dr. Kemin Zhou for his constant support, encouragement and guidance through out my masters program. The freedom that he provides his students for doing their research is unmatched. I feel very lucky to work under his invaluable tutelage.

I am sincerely thankful to Dr. Jorge Aravena for sharing his vast experience with me via mutual discussions and organized meetings. His guidance will go a long way in helping me in my professional career.

I extend my sincere thanks to Dr. Guoxiang Gu for sharing his knowledge and expertise in the form of courses and discussions. I also thank him for accepting to be in my thesis committee. I take this point to thank Dr. Marcio S. de Queiroz for offering me work in his lab in my first semester and also for his continuous moral support.

I thank Dr. Xinjia Chen for sharing his new ideas, views, and for his lengthy fruitful discussions on various topics. I thank Steve and Amy of Rassimtech for their support in using AVDS software.

I thank my colleagues and labmates Jianqiang He, Zhongshan Wu, Nike Liu, Xiaobo Li, Laurentiu Marinovici, Sivaram Venkata, Lalitha Devarakonda, Min Luo, for providing a fruitful work environment. I also want to mention my closest friends in LSU Sameer Herlekar, Charan Masarapu, Giri, and Abhilash, for their modesty, optimism and positive conversations that made my stay at LSU much more fun and enjoyable.

I owe the greatest appreciation to my parents Girija Sanker and Jaya Bharathi, my brother Lokesh, my sister Gayathri and rest of my family members for their

unconditional love, affection, and friendship.

Phalguna Kumar Rachinayani

May, 2006

# Table of Contents

Acknowledgements .....	iii
List of Tables .....	vii
List of Figures .....	viii
Notation and Symbols .....	x
List of Acronyms .....	xi
Abstract .....	xii
<b>1 Introduction .....</b>	<b>1</b>
1.1 Organization of the Thesis . . . . .	2
<b>2 Uncertainty Models .....</b>	<b>4</b>
2.1 Introduction . . . . .	4
2.1.1 Linear Fractional Transformation . . . . .	4
2.2 Linear Fractional Representation of Uncertainty . . . . .	6
2.2.1 Nominal-Dynamic System . . . . .	6
2.2.2 Norm-Bounded Parametric Uncertainties . . . . .	7
2.2.3 Polytopic Uncertainties . . . . .	8
2.3 Operating Regime Based System Uncertainty Modeling . . . . .	9
2.3.1 Generation of LFT Based Structured Uncertainty Models . . . . .	10
<b>3 Fault Detection and Isolation .....</b>	<b>13</b>
3.1 Faults Classification . . . . .	13
3.1.1 Sensor Faults . . . . .	13
3.1.2 Actuator Faults . . . . .	14
3.1.3 System Component Faults . . . . .	16
3.2 Faulty System Modeling . . . . .	16
3.3 Faults Diagnosis . . . . .	17
3.3.1 Observer-Based Residual Generation . . . . .	17
3.3.2 Fault Detection and Isolation . . . . .	18
3.3.3 Application of FDI for Linear Boeing 747 Model . . . . .	19

<b>4</b>	<b>Robust Fault Tolerant Control</b> .....	<b>21</b>
4.1	LQR Based Nominal Controller Design . . . . .	21
4.2	Robust Control Reconfiguration . . . . .	23
4.2.1	Optimal Robust Controller Design under Actuator Faults . . . . .	23
4.2.2	Optimal Robust Control with Model Uncertainty and Actuator Failures . . . . .	28
4.2.3	Application of AFTC for Linear Boeing 747 Model . . . . .	29
4.3	Passive FTC . . . . .	29
4.3.1	Reliable Controller Design . . . . .	31
4.3.2	Guaranteed Cost Robust FTC . . . . .	35
<b>5</b>	<b>Robustness and Safety Analysis</b> .....	<b>37</b>
5.1	Nonlinear System Implementation . . . . .	37
5.1.1	Lyapunov Stability for Nonlinear System . . . . .	38
5.1.2	Asymptotic Stability . . . . .	39
5.2	Stability Characterization . . . . .	39
5.3	Safety Certificates . . . . .	39
5.4	Uncertain Parameters in Switching Based Controller Reconfiguration . . . . .	41
5.5	Monte Carlo Based Robustness and Safeness Analysis . . . . .	42
5.5.1	Monte Carlo Evaluation - Simulation Setup . . . . .	43
<b>6</b>	<b>Conclusions</b> .....	<b>47</b>
	<b>Bibliography</b> .....	<b>49</b>
	<b>Appendix A Boeing Aircraft Control Surfaces</b> .....	<b>53</b>
	<b>Appendix B B747 Norm Bounded Description</b> .....	<b>57</b>
	<b>Vita</b> .....	<b>62</b>

# List of Tables

5.1	Stability characterization bounds . . . . .	40
5.2	Indicator Function . . . . .	44
A.1	Boeing 747 Control Surfaces Saturation Limits . . . . .	54

# List of Figures

1.1	Block Structure of Reconfigurable Fault Tolerant Control System . . .	3
2.1	Lower Linear Fractional Representation . . . . .	5
2.2	A polytopic system . . . . .	9
2.3	Convex hull of Considered Operating Points . . . . .	10
3.1	Fault locations in a system . . . . .	13
3.2	Typical types of sensor faults . . . . .	14
3.3	Typical types of actuator faults . . . . .	15
3.4	Multiple failures in single actuator Rudder 20% at 35 Secs and 80% at 75 Secs . . . . .	20
3.5	Multiple failures in different actuators 60% Rudder failure at 75 Secs and 40% Aileron failure at 150 Secs . . . . .	20
4.1	Reconfiguration mechanism with bank of controllers . . . . .	23
4.2	Roll angle ( $\phi$ ) response with both Nominal Controller ( <i>dashed</i> ) and Robust Controller ( <i>solid</i> ) for Rudder failure of different fault intensities	30
4.3	Roll angle response with nominal controller ( <i>dashed</i> ) and Robust controller ( <i>solid</i> ) with 60% Rudder failure at 80 seconds and 40% Aileron failure at 150 seconds . . . . .	30
4.4	Eigen Values of $(\mathcal{A} + \hat{\mathcal{B}}_i K_{ri})$ for all $\varepsilon_i \in [0, 90\%]$ of Rudder failure . . .	34
5.1	Stability in the sense of Lyapunov . . . . .	38
5.2	Stability region considering state derivatives . . . . .	40
5.3	A safety certificate showing safe $\mathcal{X}_s$ and unsafe $\mathcal{X}_u$ regions . . . . .	41
5.4	Detection time delay $t_d$ . . . . .	42
5.5	Nonlinear system stability derivatives . . . . .	44
5.6	Nonlinear system states . . . . .	45

5.7	Robustness profile for Elevator with multiple controllers and no switching delay . . . . .	46
5.8	Robustness profile for Elevator with multiple controllers and 5secs switching delay . . . . .	46
A.1	Linear Actuator 658D100 for Rudder trim surface (Eaton Corporation)	53
A.2	Measurements of Linear Actuator 658D100 for Rudder trim surface (Eaton Corporation) . . . . .	54
A.3	Airplane actuators definition and function (NASA Glenn Research Center website) . . . . .	55
A.4	Boeing 747 Three View [15] . . . . .	56

# Notation and Symbols

$\mathbb{R}$	field of real numbers
$\mathbb{C}$	field of complex numbers
$\mathcal{F}_l(\cdot, \cdot)$	lower LFT
$\mathcal{F}_u(\cdot, \cdot)$	upper LFT
$\Delta$	set of uncertain parameters
$\text{diag}(a_1, \dots, a_n)$	an $n \times n$ diagonal matrix with $i^{\text{th}}$ diagonal element $a_i$
$A^T$	transpose
$I(\cdot)$	indicator function
$\Omega(\cdot)$	convex hull
$\ A\ $	spectral norm of A
$\Xi$	nonlinear system
$\text{Ker}(A)$	kernel or null space of A
$\mathcal{X}_u$	unsafe set
$\mathcal{X}_s$	safe set
$\mathcal{K}$	Controller set
$\Upsilon$	Robustness evaluation integral

# List of Acronyms

FTC	Fault Tolerant Control
FDI	Fault Detection and Isolation
PBH	Popov-Belevitch-Hautus
ARE	Algebraic Riccati Equation
LMI	Linear Matrix Inequality
YALMIP	Yet Another LMI Parser

# Abstract

The need to design controllers that guarantee both stability and performance upon the occurrence of faults has been an active area of research. To address this problem, in this thesis we present different methodologies to design robust controllers that guarantee both stability and robustness for actuator faults and uncertainties. In the first part of this thesis, we introduce the classical uncertainty formulation using Linear Fractional Transformation (LFT) and describe LFT's special cases-norm bounded and convex polytopic uncertainty descriptions. Practical methods to formulate these uncertainty structures are described. In the same spirit, formulation of faults and their modeling for robust control system design is provided.

In the second part of this thesis, we demonstrate the application of a Luenberger observer for fast Fault Diagnosis and Isolation (FDI). We describe the methodology to design a robust optimal control for actuator faults and present controller reconfiguration mechanism based on switching for the design of Fault Tolerant Control (FTC). System with both norm bounded uncertainties and actuator faults is formulated and an analytic method to find a robust stabilizing and guaranteed cost reliable controllers are also mentioned.

To the end, we implement designed linear controllers in Boeing 747 (B747) nonlinear system. We also define and evaluate potential problems that arise in switching based FTC and their effect on the closed loop nonlinear system. Robustness of linear controllers in nonlinear B747 was evaluated using excessive Monte Carlo simulation and results are presented.

# Chapter 1

## Introduction

Fault Tolerant Control (FTC) for aircraft systems has received considerable attention from the control engineers in the past couple of decades. The inspiration behind this attention is to build safer and more reliable aircraft systems that can sustain the effect of failures. The need for fault tolerant control methods is therefore critical.

A fault is defined as a “malfunction” of any physical component or a sub-system that results in its failure to perform as designed. The main reasons for faults in aircraft systems are:

- Natural wear and tear of mechanical or electrical components,
- External unknown catastrophic disturbances, and
- Improper maintenance of electro-mechanical components.

It is highly desired that when a fault occurs, it is timely detected and is informed to both pilot and autopilot to take necessary action. This timely response to faults reduces any disastrous consequences. For this reason, fault detection and isolation methods received considerable attention from both control and signal processing communities in the last couple of decades (see [14, 11] for an extensive survey on various methods for fault detection).

After a fault is detected, a corrective action should be taken by the autopilot to guarantee both closed loop stability and performance. The two methods for designing fault tolerant control systems (FTCS) in control literature are passive and active methods. Passive FTCS methods (PFTCS), also known as reliable control systems

[20, 36], rely on robust control system framework and the controller is designed to compensate a set of predefined worst case faults. On the other hand, in active FTCS (AFTCS) also known as reconfigurable control system (shown in Figure 1.1) the control law is redesigned for every fault situation. The control law redesign is carried out either by online adaptation or by selecting a pre-designed controller from a bank of controllers (projection method). Refer to [8, 11, 25, 42] and references therein for a brief survey of available PFTCS and AFTCS methods.

Faults being dynamic in nature, the reconfiguration method should be capable of accommodating them quickly, especially for complex systems like aircrafts. Reconfiguration based on adaptive techniques [7] demands a fast detection and isolation of a fault and is computationally involved. Although this approach claims to guarantee stability for all kinds of faults, the computational complexity of the algorithm increases with increasing complexity of the system. This computational complexity restricts the application of adaptive methods for controller reconfiguration in a more complex system like an aircraft system. On the other hand, reconfiguration based on selection of a controller from a pre-designed set of controllers, generally known as *bank of controllers approach* is more realistic, as the controllers are designed considering the most likely faults [8, 18, 19]. This method has low computational complexity making it more practical for complex systems like an aircraft.

## 1.1 Organization of the Thesis

This thesis is organized following the block structure of a fault tolerant control system shown in Figure 1.1. In Chapter 2, we describe various uncertainty modeling methods used in robust control community. Linear Fractional Transformation (LFT) is described along with norm bounded structured parameter uncertainty and convex polytopic uncertainty descriptions. A single norm bounded uncertain parameter model that can describe a certain flight envelope is identified.

Chapter 3 begins with the definition of various fault types in aircraft systems along with their formulation. This chapter also introduces a fault detection and isolation mechanism for actuator faults using Luenberger observer.

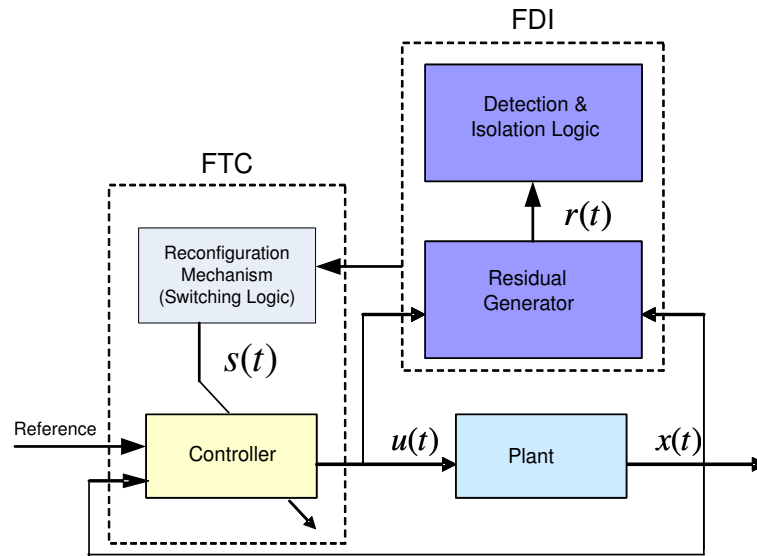


Figure 1.1: Block Structure of Reconfigurable Fault Tolerant Control System

Chapter 4 describes methodologies for designing fault tolerant control systems. First, we design a nominal controller that guarantees performance in no fault situation. Then we present reconfigurable controller design method for single and multiple actuator faults that are optimal and guarantee stability of the linear closed loop. Passive guaranteed cost reliable controller design method for system with both uncertainties and actuator faults is also described in this chapter.

In Chapter 5, we implement the designed linear robust controllers in a nonlinear aircraft system. Stability characterization and safety certificates are described for nonlinear Boeing 747 aircraft model. Then, we evaluate stability and safeness of the closed loop with linear controllers using Monte Carlo based probabilistic methods.

Chapter 6 are conclusions of this thesis.

# Chapter 2

## Uncertainty Models

### 2.1 Introduction

When robustness requirement is imposed in the controller design process, considering relevant uncertainty structure with specified uncertainty bounds is of primary importance. Uncertainty is defined as the difference between real-system and a mathematical model. Upon designing, a robust controller guarantees robustness property in the considered uncertainty set [40]. In modern flight control problems, a robust controller is designed to guarantee robustness for a particular flight envelope.

Varying flight conditions effect various parameters of an aircraft system. In robust control theory of aircraft systems, a particular flight envelope is represented as uncertainty with predefined bounds [5]. For this reason, in this chapter we briefly note the classical uncertainty formulation method using Linear Fractional Transformations (LFTs) and describe norm-bounded and polytopic uncertainties which are special cases of LFTs. Both norm-bounded and polytopic uncertainty structures enable the designer to use different mathematical tools to solve the problem at hand [3, 22]. In addition, we discuss some methods available in literature used for generation of norm-bounded and convex polytopic uncertainty structures.

#### 2.1.1 Linear Fractional Transformation

Usage of Linear Fractional Transformation (LFT) framework for system realization, analysis and synthesis of uncertain systems is common in the robust control literature.

The main advantage of LFT framework is that it enables to formulate any interconnected system into one general framework that can be used for both analysis and synthesis purposes. In this section, we give a brief overview to LFT framework. For a more detailed description of LFT framework and its various applications in robust control refer to [23, 40]. A complex transfer matrix  $M \in \mathbb{C}^{(p_1+p_2) \times (q_1+q_2)}$  partitioned as

$$M = \begin{bmatrix} M_{11} & M_{12} \\ M_{21} & M_{22} \end{bmatrix} \quad (2.1)$$

interconnected with some complex matrix  $\Delta_l \in \mathbb{C}^{(p_1 \times q_1)}$  or  $\Delta_u \in \mathbb{C}^{(p_2 \times q_2)}$  can be represented either as a lower LFT or as an upper LFT. Figure 2.1 represents the interconnection between  $M$  and  $\Delta_l$  in lower LFT form. The mathematical representations of both lower and upper LFTs are given as:

$$\mathcal{F}_l(M, \Delta_l) = M_{11} + M_{12}\Delta_l(I - M_{22}\Delta_l)^{-1}M_{21} \quad (2.2)$$

$$\mathcal{F}_u(M, \Delta_u) = M_{22} + M_{21}\Delta_u(I - M_{11}\Delta_u)^{-1}M_{12} \quad (2.3)$$

where  $\mathcal{F}_l(.,.)$  and  $\mathcal{F}_u(.,.)$  represents lower and upper LFTs. In formulating a con-

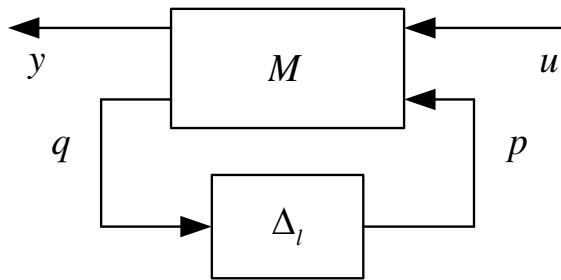


Figure 2.1: Lower Linear Fractional Representation

nected system into either lower  $\mathcal{F}_l(M, \Delta)$  or upper  $\mathcal{F}_u(M, \Delta)$  LFT framework the LFT should satisfy causality and well-posed condition for any  $\Delta$ . Using LFTs, we can formulate many kinds of problems in control literature. For example when  $\Delta = \frac{1}{s}I$ , we can represent a transfer matrix in an LFT form shown in the following example.

**Example 1.** [13]  $\mathcal{F}_u \left( \begin{bmatrix} A & B \\ C & D \end{bmatrix}, \frac{1}{s}I \right) = D + C(sI - A)^{-1}B.$

We can also formulate other mathematical objects such as polynomials, rational functions, parametric uncertainties and many more. In the next section we consider usage of LFT in formulating a system with parametric uncertainties and for more details about other formulation refer to [40].

## 2.2 Linear Fractional Representation of Uncertainty

The main motivation of discussing parameter uncertainty in this section is changes in flight condition in a particular flight envelope effects various physical parameters of an aircraft. As discussed earlier section, LFT framework provides a mechanism to construct a dynamic system with varying parameters.

Now supposing  $\Delta$  representing parameter uncertainty with some structure (to be discussed in Section 2.2.2), the interconnected system in Figure 2.1 with  $\Delta$  entering in feedback fashion can be described using state-space matrices as

$$\begin{aligned} \dot{x}(t) &= Ax(t) + Bu(t) + Fp(t), & x(0) &= x_0 \\ y(t) &= Cx(t) \\ q(t) &= E_1x(t) + E_2u(t) \\ p(t) &= \Delta q(t) \end{aligned} \tag{2.4}$$

where  $x(t) \in \mathbb{R}^n$  is the state vector,  $y(t) \in \mathbb{R}^{n_y}$  is the output vector,  $u(t) \in \mathbb{R}^{n_u}$  is the control vector,  $p(t) \in \mathbb{R}^{n_p}$  and  $q(t) \in \mathbb{R}^{n_q}$  are uncertainty vectors, and  $A, B, C, F, E_1, E_2$  are real matrices with appropriate dimensions.

### 2.2.1 Nominal-Dynamic System

A nominal model is assumed to be free from the influence of uncertainty and is useful when conducting model-based designs. Mathematically, it can be realized by assuming no uncertainty i.e.,  $\Delta = 0$  in (2.4). The resultant nominal LTI system has transfer function given as

$$G(s) = D + C(sI - A)^{-1}B. \tag{2.5}$$

## 2.2.2 Norm-Bounded Parametric Uncertainties

In this subsection we give a general description of norm-bounded parametric uncertainties. The uncertainty system  $G(\Delta)$  with uncertainties in state and input matrices given in (2.4) is represented as:

$$\dot{x}(t) = (A + F\Delta E_1)x(t) + (B + F\Delta E_2)u(t) \quad (2.6)$$

where  $E_1, E_2$  are input uncertainty structure and  $F$  is the output uncertainty structure. Identification procedure of uncertainty structure matrices  $E_1, E_2$  and  $F$  is given in Section 2.3.1. The uncertainty  $\Delta$  in (2.6) is assumed to belong to norm-bounded structured uncertainties set  $\mathbf{\Delta}$  i.e.,

$$\|\Delta\| \leq 1, \Delta \in \mathbf{\Delta}.$$

The parameter uncertainty set  $\mathbf{\Delta}$  is represented as:

$$\mathbf{\Delta} = \{block\ diag(\delta_1 I_{k_1}, \dots, \delta_s I_{k_s}, \Delta_1, \dots, \Delta_f) : \delta_i \in \mathbb{R}, \Delta_i \in \mathbb{R}^{k_{s+i} \times k_{s+i}}\}. \quad (2.7)$$

When the structure of uncertainty is known (described in Section 2.3.1), the conservativeness introduced by unstructured uncertainty is reduced by considering the structure information and introducing a scaling set of the form:

$$\mathcal{S} = \{block\ diag(S_1, \dots, S_f, s_1 I_{k_1}, \dots, s_s I_{k_s}) : s_i \in \mathbb{R}, S_i \in \mathbb{R}^{k_i \times k_i}, s_i > 0, S_i > 0\}. \quad (2.8)$$

For each  $S \in \mathcal{S}$ , we have

$$\Delta S = S \Delta \quad \forall \Delta \in \mathbf{\Delta}. \quad (2.9)$$

The freedom in the selection of  $S \in \mathcal{S}$  is used to reduce the conservativeness.

The following lemma is a simple matrix fact and is used in design of robust controllers described in Chapter 4.

**Lemma 1.** *[Completion of Squares] The following inequality*

$$H^T \Delta^T F + F^T \Delta H \leq H^T S^{-1} H + F^T S F \quad (2.10)$$

holds for all  $\Delta \in \mathbf{\Delta}, S \in \mathcal{S}$ .

*Proof.* It is always true that

$$\begin{aligned} (S^{1/2}F - S^{-1/2}\Delta H)^T(S^{1/2}F - S^{-1/2}\Delta H) &\geq 0 \\ \text{i.e., } H^T\Delta^T S^{-1}\Delta H + F^T S F &\geq H^T\Delta^T F + F^T\Delta H \end{aligned}$$

But for all  $\Delta \in \mathbf{\Delta}$

$$\|\Delta\| \leq 1 \Leftrightarrow \Delta^T\Delta \leq I$$

and with  $S \in \mathcal{S}$  and using (2.9)

$$H^T\Delta^T F + F^T\Delta H \leq H^T\Delta^T S^{-1}\Delta H + F^T S F \leq H^T S^{-1}H + F^T S F.$$

□

### 2.2.3 Polytopic Uncertainties

It is a known fact that by defining a system with polytopic uncertainties the optimum value either maximum or minimum of a cost function lies on one of the vertex of the polytope.[9]. The advantage of polytopic system formulation is that there are many efficient convex optimization based computation tools that can solve both analysis and design problem. In a polytopic model uncertainty description, the state-space matrices of the system are known to lie in a given polytope. As mentioned earlier, polytopic uncertainties can be considered as a special case of LFT uncertainty model (2.4).

We now give the description of a system using convex polytopic uncertainties. In the polytopic uncertainty description, it is assumed that the origin (nominal model) is inside the polytope (illustrated in Figure 2.2). The polytopic uncertainty system with uncertainties in state and input matrices is described as:

$$\begin{aligned} \dot{x}(t) &= A(\theta)x(t) + B(\theta)u(t), \quad x(0) = 0, \\ y(t) &= Cx(t) \end{aligned} \tag{2.11}$$

where the convex coordinates  $\theta \in \mathbb{R}^L$  is the uncertain parameter vector. The convex hull  $\Omega$  affine in  $\theta$  is defined as:

$$\begin{aligned} \Omega(\theta) \equiv \begin{bmatrix} A(\theta) & B(\theta) \end{bmatrix} &= \begin{bmatrix} A_0 & B_0 \end{bmatrix} + \sum_{i=1}^L \begin{bmatrix} A_i & B_i \end{bmatrix} \theta_i \\ &= \Omega_0 + \sum_{i=1}^L \Omega_i \theta_i \end{aligned} \tag{2.12}$$

where  $\theta_i \in [0, 1]$  and  $\sum_{i=1}^L \theta_i = 1$ .

The computational complexity of the problem with polytopic uncertainties depends on the number of vertices  $L$  of the considered convex polytope [6]. When  $L$  is large, many computational tools suffer from the curse of dimensionality and may not perform well. In the next section we give some practical methods of formulating both norm-bounded

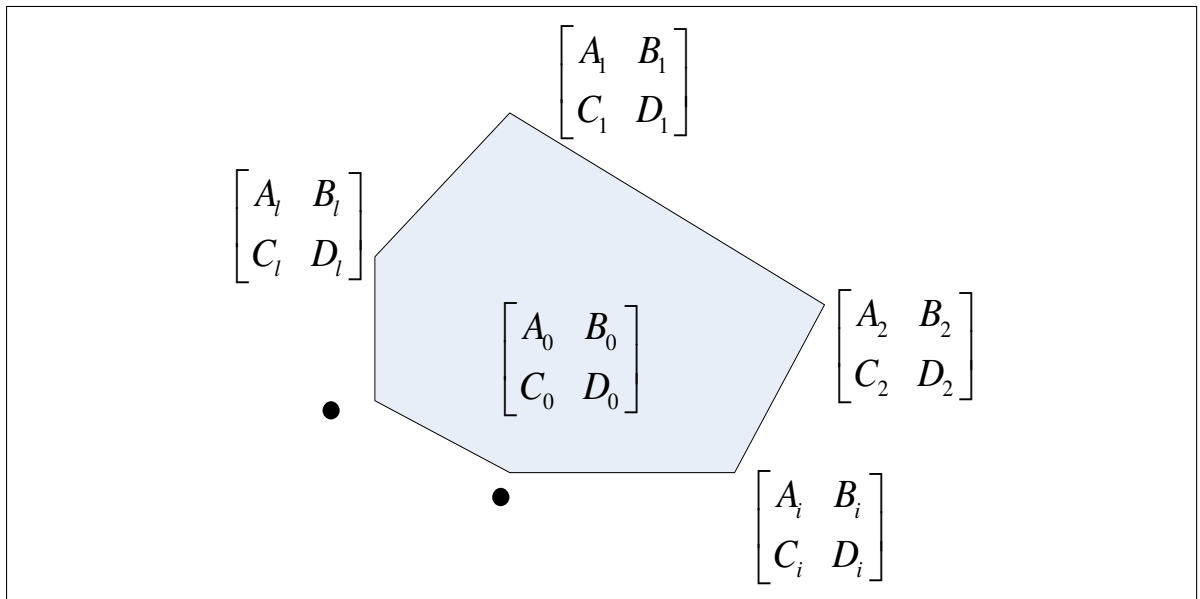


Figure 2.2: A polytopic system

and polytopic uncertainties.

## 2.3 Operating Regime Based System Uncertainty Modeling

In controlling complex systems, to borrow words from Smith and Johansen [34], *In everyday life as well as in solving engineering problems, the standard approach to complex problem solving is the divide-and-conquer strategy: A complex problem is some how partitioned into a number of simpler subproblems that can be solved independently, and whose individual solutions yield the solution of the original complex problem.*

One of the major problems in design of flight control systems is modeling uncertainties and parameter variations in characterizing an aircraft and its operating

environment. An aircraft flight path is specified by the operating conditions or trimming conditions. Changes in operating conditions results in change of aerodynamic coefficients and will lead to variation in flight dynamics. In this thesis a particular set of flight conditions are considered with bounded parameter variations. The parameters used to trim the flight in a straight and level flight path are true air speed  $V_{TAS} \in [230m/sec, 245m/sec]$ , flight path angle  $\gamma \in [-10deg, +10deg]$ , and height  $h \in [6000m, 10000m]$  which form a bounding box as shown in Figure 2.3. The true operating points of the aircraft lies inside the bounding box and a convex hull representing the operating points is also shown in Figure 2.3.

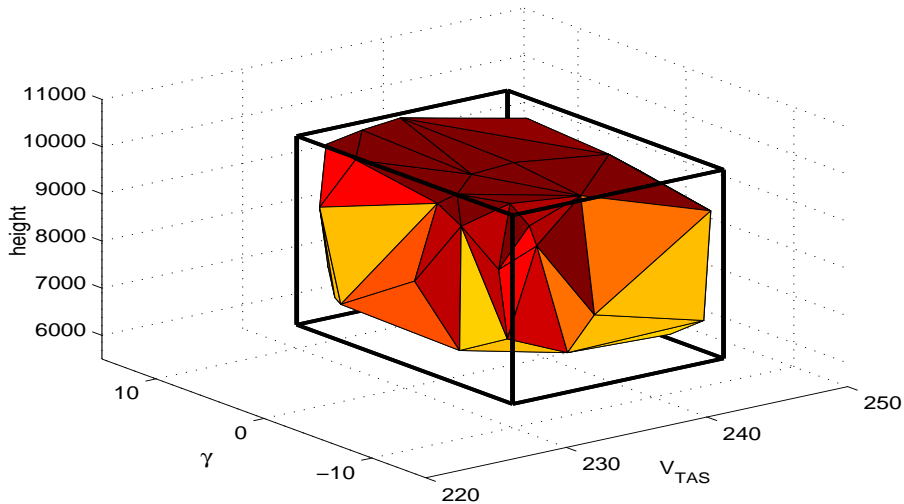


Figure 2.3: Convex hull of Considered Operating Points

### 2.3.1 Generation of LFT Based Structured Uncertainty Models

After discussing the LFT formulation along with uncertainty representation we now provide a method for identifying the structure of parameter uncertainty in this subsection. The construction of LFT based structured uncertainty models received considerable attention in the robust aircraft control community in the last decade. The main advantage of this type of uncertainty formulation is the advantage of applying

various robust control methods. For a detailed discussion of various methods available in the literature to generate an LFT based structured uncertainty for aircraft systems refer to [35, 5]. Many methods in the norm-bounded uncertainty structure identification literature requires the designer to have apriori information about the influence of uncertainty on the dynamics of the system. In this section, we describe a “black box” approach for LFT based structured uncertainty generation method [5]. In a black box approach, numerical linearizations are repeatedly performed at several operating points by varying a parameter vector  $p \in \mathbb{R}^n$ . The parameter vector  $p$  defines a flight envelope where each parameter  $p_i \in [p_i^{min}, p_i^{max}]$ ;  $\forall i \in n$ . Upon linearizing at different operating points we get a multi-model state description of the form :

$$\delta \dot{x}(t) = A_i \delta x(t) + B_i \delta u(t). \quad (2.13)$$

For the above system matrices that describes a flight envelope, lower and upper bounds of every entry in all system matrices are identified. Let  $A^{min}$  and  $A^{max}$  represents matrices with lower and upper bounds for the all the entries of  $A_i$ ;  $i = 1, \dots, n$ . Then each entry  $(j, k)$  can be replaced by a single entry of the form

$$a_{j,k} = a_{j,k}^0 + s_l \delta_i, \quad (2.14)$$

where  $a_{j,k}^0 = (a_{j,k}^{min} + a_{j,k}^{max})/2$  is the mean nominal value,  $s_l = (a_{j,k}^{max} - a_{j,k}^{min})/2$  is the slope of the corresponding to element  $(j, k)$ . If  $s_l \neq 0$  then the uncertainty parameter  $|\delta_i| \leq 1$ . Now an affine parameter dependent model can be constructed of the form :

$$\delta \dot{x}(t) = A_{pA} \delta x(t) + B_{pB} \delta u(t) \quad (2.15)$$

where the state matrices are of the form

$$\begin{bmatrix} A_{pA} & B_{pB} \end{bmatrix} = \begin{bmatrix} A_{p0} & B_{p0} \end{bmatrix} + \sum_{i=1}^{n_A} \delta_i \begin{bmatrix} A_{pi} & 0 \end{bmatrix} + \sum_{i=n_A+1}^{n_B} \delta_i \begin{bmatrix} 0 & B_{pi} \end{bmatrix}$$

where  $n_A$  and  $n_B$  are the number of uncertain parameters in state matrix  $A$  and input matrix  $B$ . Now, each of the matrices associated with each  $\delta_i$  is factored into row and

column vectors of the form  $A_{pi} = E_i \Delta_A F_i$  with  $\Delta_A = \begin{bmatrix} \delta_1 & & \\ & \ddots & \\ & & \delta_{nA} \end{bmatrix}$ . Matrices  $E_i$  and  $F_i$  represent the output and input uncertainty structures and it can be written as (2.4).

Now we give an illustrative example of identifying norm bounded structured uncertainty for a given set of state matrices.

**Example 2.** *Let*

$$A_1 = \begin{bmatrix} 1 & 2 \\ 0.1 & -0.2 \end{bmatrix}, A_2 = \begin{bmatrix} -0.1 & 2 \\ 0.9 & 3 \end{bmatrix}, A_3 = \begin{bmatrix} 1.1 & 2 \\ 0.5 & 2 \end{bmatrix}$$

be three state matrices in  $A_p$  of linearized models obtained for three different parameter values. Now using the black box method mentioned in Section 2.3.1 we can represent in the form given in (2.14) as :

$$A_p = \begin{bmatrix} 0.5 & 2 \\ 0.5 & 1.4 \end{bmatrix} + \delta_1 \begin{bmatrix} 0.6 & 0 \\ 0 & 0 \end{bmatrix} + \delta_2 \begin{bmatrix} 0 & 0 \\ 0.4 & 0 \end{bmatrix} + \delta_3 \begin{bmatrix} 0 & 0 \\ 0 & 1.6 \end{bmatrix}$$

where uncertain parameters  $\delta_i; i = 1, 2, 3$  satisfy  $|\delta_i| \leq 1$ . Rewriting the above into

$$A_p = \begin{bmatrix} 0.5 & 2 \\ 0.5 & 1.4 \end{bmatrix} + \begin{bmatrix} 0.6 & 0 & 0 \\ 0 & 0.4 & 1.6 \end{bmatrix} \begin{bmatrix} \delta_1 & & \\ & \delta_2 & \\ & & \delta_3 \end{bmatrix} \begin{bmatrix} 1 & 0 \\ 1 & 0 \\ 0 & 1 \end{bmatrix}$$

$$A_p = A_0 + E_1 \Delta F_1.$$

Now we give a simple example that demonstrates the usage of polytopic system and solving multiple inequalities in a Lyapunov inequality to obtain a stabilizing solution. The problem is solved using YALMIP toolbox.

**Example 3.** *In this example we solve a Lyapunov inequality*

$$A_i^T P + P A_i < I, \tag{2.16}$$

where  $A_i$  are mentioned in the above Example 2 and  $P = P^T$  is the variable. The solution to the Lyapunov inequality (2.16) is obtained as

$$P = \begin{bmatrix} 0.1733 & -0.0800 \\ -0.0800 & 0.1336 \end{bmatrix}.$$

The procedure mentioned in the above Example 3 of solving LMIs at various vertices of a polytope will be used in Corollary 1 of Chapter 4.

# Chapter 3

## Fault Detection and Isolation

In this chapter, we describe faults in an aircraft system and provide their models. After modeling of faults, we implement a fault detection and isolation mechanism using Luenberger observer for a linear Boeing 747 model.

### 3.1 Faults Classification

Faults occur at different locations of a system and are classified according to the location of their occurrence. As shown in Figure 3.1, faults occur in sensors, actuators and the system itself.

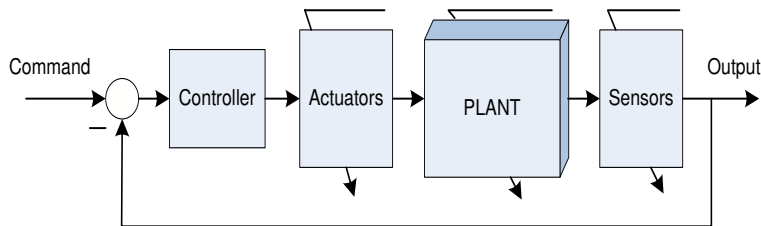


Figure 3.1: Fault locations in a system

#### 3.1.1 Sensor Faults

A system with sensor faults results in a wrong measurement signal  $y(t)$  which is used in filter design. Some typical types of sensor faults shown in Figure 3.2 are mathematically represented as [8]:

- Bias:  $y_i(t) = x_i(t) + d_i$  where disturbance  $\dot{d}(t) = 0, d_i(t_F) \neq 0$ ,

- Drift:  $y_i(t) = x_i(t) + d_i(t)$  where  $d_i(t) = \lambda_i t$ ,  $(0 < \lambda_i < 1, \forall t \geq t_F)$ ,
- Loss of Accuracy:  $y_i(t) = x_i(t) + d_i(t)$  where  $|d_i(t)| \leq d_i$ ,  $\dot{d}_i \rightarrow 0 \forall t \geq t_F$ ,
- Freezing:  $y_i(t) = x_i(t_F) \forall t \geq t_F$ .

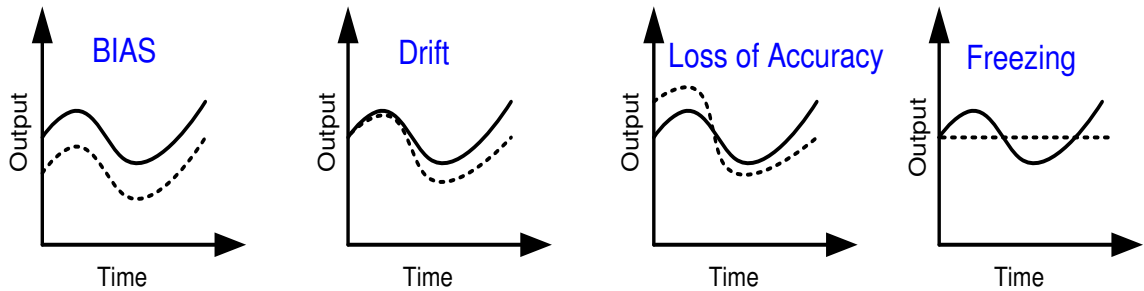


Figure 3.2: Typical types of sensor faults

Modern aircraft systems are highly instrumented with multiple redundant sensors measuring directly or indirectly all of the system state variables. Now we make the following assumption about the retrieval of system states  $x(t)$  from the given nominal LTI model (2.5).

**Assumption 3.1.**  $p \geq n$  and  $C$  has full column rank, i.e.,  $\text{rank}(C) = n$ .

Assumption 3.1 implies that system states are available and can, for example, be obtained by

$$x(t) = C^+ y(t)$$

where  $C^+$  is the left pseudo inverse of  $C$ . This assumption is quite common in modern flight control systems. The importance of Assumption 3.1 will be discussed in the fault diagnosis section.

### 3.1.2 Actuator Faults

Actuators are the last components in the control-action implementation and play an important role in delivering the necessary power to manipulate the controlled variable. Most of the actuators in a modern aircraft system are either hydraulic or pneumatic powered systems. Due their power delivering capability actuators are generally huge and bulky in nature (see Appendix A for an example). The size

and weight of individual actuator, limits the capability of having multiple redundant actuators to manipulate the same variable in an aircraft system. So consideration of actuator faults has been an active area of research in the past couple of decades [7, 24, 38]. Figure 3.3 shows some typical types of actuator faults in aircraft systems. In the following, we describe the mathematical representation of each type of actuator faults.

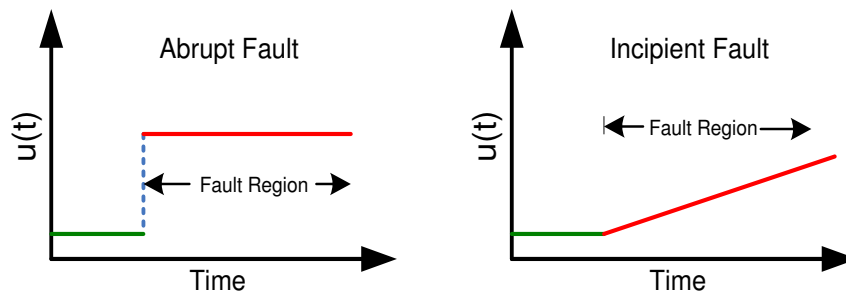


Figure 3.3: Typical types of actuator faults

- Abrupt Faults:** Abrupt faults are “hard” faults and have a large influence on the control action. Abrupt faults generally occur due to electric short circuits or sudden damage of control surface due to environmental factors. Due to their sudden changing nature, abrupt faults are easy to detect upon occurrence. Sudden actuator struck is a typical type of abrupt fault and is represented as  $u_F(t) = u(t) - \varepsilon u(t_F)$  where  $\varepsilon \in [-1, 1]$ ,  $\forall t \geq t_F$ . Here when  $\varepsilon \in [0, 1]$  the fault results in loss of control effector efficiency and when  $\varepsilon \in [-1, 0]$  an additional unwanted faulty control effort is fed into the control loop.
- Incipient Faults:** Incipient faults are soft faults and have a considerable effect on the control-action in the long run. These faults generally occur due to leaks in hydraulic or pneumatic systems. Due to a slow change in the magnitude of incipient faults, they are hard to detect.  $u_F(t) = u(t) + su(t_F)$  where slope  $s = \frac{u(t_F)}{t_F}$ ,  $\forall t \geq t_F$

### 3.1.3 System Component Faults

Component faults generally change the elements of the system matrices and aerodynamic coefficients. Due to the distributed nature of components in a large-scale systems like aircraft systems, component faults are hard to detect and identify. Consideration of component faults is important in high-performance aircrafts like war-planes due frequent structural damage. As our concentration in this thesis is on commercial plane (Boeing 747), we will not concentrate on component faults.

## 3.2 Faulty System Modeling

We assume that the actuator faults are modeled as *additive* errors which results in loss of gain in the actuator signals:

$$\dot{x}(t) = Ax(t) + Bu(t) + Bf_a(t), \quad (3.1)$$

where  $f_a \in \mathbb{R}^m$  indicates the vector of actuator faults. The  $i^{th}$  element of  $f_a$  is of the form  $-\varepsilon_i u_i$  with  $\varepsilon_i \in [0, \varepsilon_{imax}]$ ,  $i = 1, \dots, m$  and  $\varepsilon_{imax} \leq 1$ . Here,  $\varepsilon_i = 0$  implies a no fault situation and  $\varepsilon_i = \varepsilon_{imax} = 1$  implies a full fault situation or complete  $i^{th}$  actuator outage situation.

In active fault tolerant control (to be discussed in Chapter 4) we use reconfiguration mechanism and distribute the control action to different actuators for closed loop fault accommodation. By transferring control effort to other actuators, there is a possibility that a single actuator failure may result in multiple simultaneous actuator failures due to additional load on non faulty actuators [7, 33]. Due to this reason in this thesis we consider both single and multiple actuator failure cases. Now we give the representation of both single and multiple simultaneous actuator faults used in this thesis.

**Single Actuator Fault:** The control input matrix for  $i^{th}$  actuator worst case failure  $\varepsilon_{imax}$  is represented as

$$B_{imin} = B(I - e_i e_i^T \varepsilon_{imax}). \quad (3.2)$$

**Multiple Actuator Faults:** The control input matrix with multiple simultaneous worst case actuator faults  $\varepsilon_{imax}$  where  $i \in \mathcal{K}$  is represented as

$$B_{min} = B(I - \sum_{i \in \mathcal{K}} e_i e_i^T \varepsilon_{imax}) \quad (3.3)$$

or as

$$B_{min} = B \prod_{i \in \mathcal{K}} (I - e_i e_i^T \varepsilon_{imax}).$$

For fault  $\varepsilon_i \leq \varepsilon_{imax}$  the above can be represented as

$$\hat{B} = B(I - \sum_{i \in \mathcal{K}} e_i e_i^T \varepsilon_i).$$

### 3.3 Faults Diagnosis

The first step in Fault Diagnosis (FD) is residual generation (shown in Figure 1.1). There has been a considerable research done on the techniques used to generate residuals and their application in FD. Some of the widely available techniques in the literature are based on parity space approach, dedicated observer-based approach and fault detection filter approach (see [11, 14, 25]) for an extensive study on various approaches.

**Definition 1. Residual signal:** A diagnostic signal  $r(t)$  with property  $\|r(t)\| = 0$  (almost negligible) under no fault situation and  $\|r(t)\| \neq 0$  upon the occurrence of a fault.

#### 3.3.1 Observer-Based Residual Generation

Observer based residual generation is simple and reliable to implement in practical applications. In this subsection we propose the procedure for designing a dedicated observer and the associated residual generator.

A Luenberger observer of the form

$$\dot{\hat{x}}(t) = A\hat{x}(t) + Bu(t) + L(y(t) - C\hat{x}(t)) \quad (3.4)$$

is considered for residual generator design, here  $L$  is the observer gain matrix such that  $A - LC$  is stable.

Now define error between output and estimated output

$$e(t) = y(t) - C\hat{x}(t). \quad (3.5)$$

The following theorem provides a method for designing a residual generator.

**Theorem 1.** [41] *Let  $\alpha \geq 0$  be a suitably chosen large number. Let  $\hat{x}(0) = x(0)$  and the observer gain be*

$$L = (A + \alpha I)C^+. \quad (3.6)$$

*Then the actuator faults  $f_a(t)$  can be detected and isolated by the following residual generator*

$$r(t) = \alpha B^+ C^+ e(t) \quad (3.7)$$

*where  $B^+$  and  $C^+$  are left pseudo inverses of  $B$  and  $C$ .*

*Proof.* First of all, since  $C$  has full column rank (Assumption 3.1),  $x(t)$  is available for all instants of time. Hence it is possible to choose  $\hat{x}(0) = x(0)$ . Now let the state error be  $e_x = x - \hat{x}$ . Then  $e_x(0) = 0$  and

$$\begin{aligned} \dot{e}_x(t) &= (A - LC)e_x(t) + Bf_a(t) = -\alpha e_x(t) + Bf_a(t) \\ e(t) &= Ce_x(t). \end{aligned}$$

Therefore, the residual signal can be generated using the error signal as

$$\begin{aligned} r(t) &= \alpha B^+ C^+ e(t) = \alpha B^+ C^+ C \int_0^t e^{-\alpha(t-\tau)} Bf_a(\tau) d\tau \\ &= \alpha \int_0^t e^{-\alpha(t-\tau)} f_a(\tau) d\tau. \end{aligned}$$

It is now clear that all actuator faults are clearly detected and isolated from the residual function  $r(t)$ .  $\square$

**Remark 3.1.** *It is clear from the above proof and discussion that the choice of  $\alpha$  plays an important role in the speed of fault detection. It is desirable to choose a large  $\alpha$  ( $\gg 0$ ). However, this is limited by the system bandwidth.*

### 3.3.2 Fault Detection and Isolation

The next step after residual generation in FTC is the analysis of the residual signal for faults. Different analysis procedures are used depending on the techniques used to generate the residual signal. The widely used approach for analyzing the residual signal generated by dedicated observers to determine faults is *threshold logic* or *limit monitoring* [11, 14]. Threshold logic is also known as *Hysteresis Constant* in switching control literature [21].

A simple threshold logic for analysis of the residual signal is:

$$\begin{cases} \|r_i(t)\| < T_i & \text{for no fault condition} \\ \|r_i(t)\| \geq T_i & \text{for fault condition} \end{cases} \quad (3.8)$$

where  $r_i(t)$  and  $T_i$  are the residual signal and the predefined threshold level for the  $i^{\text{th}}$  actuator,  $i \in m$ .

**Remark 3.2.** *As an observer based residual generator methodology considers either system states or outputs for the generation of residual signal,  $\|r(t)\|$  depends on  $\|x(t)\|$ . In regulator case  $\|x(t)\| \rightarrow 0$ ,  $\|r(t)\|$  takes a small magnitude.*

### 3.3.3 Application of FDI for Linear Boeing 747 Model

The FDI mechanism method described in previous sub-sections is used to detect and isolate actuator faults in a linear Boeing 747 model and the results are presented in this section. The residual signal  $r(t)$  in (3.7) is a function of actuator fault  $f_a(t)$ . Abrupt faults of different intensities are considered in both single and multiple actuators. To detect actuator faults, multiple threshold levels can be considered for each actuator. The threshold level selection methods are generally problem specific and is not useful for a general case. There are few methods based on signal processing techniques, fuzzy logic based techniques in the literature which are used to design optimal threshold levels (see [14, 32]). To avoid missed alarms or improper fault detection, threshold levels selection is done on the basis of designer's experience and the problem requirements. Figure 3.4 illustrates the residual signal for a system with multiple fault intensities in the same actuator and Figure 3.5 for different actuators. In the simulation result  $\alpha$  in (3.7) is selected to have value 10.

**Remark 3.3.** *The switching mechanism switches to the corresponding robust controller designed considering the fault intensity. And will remain in the closed loop resulting in the residual  $\|r(t)\| \rightarrow 0$ .*

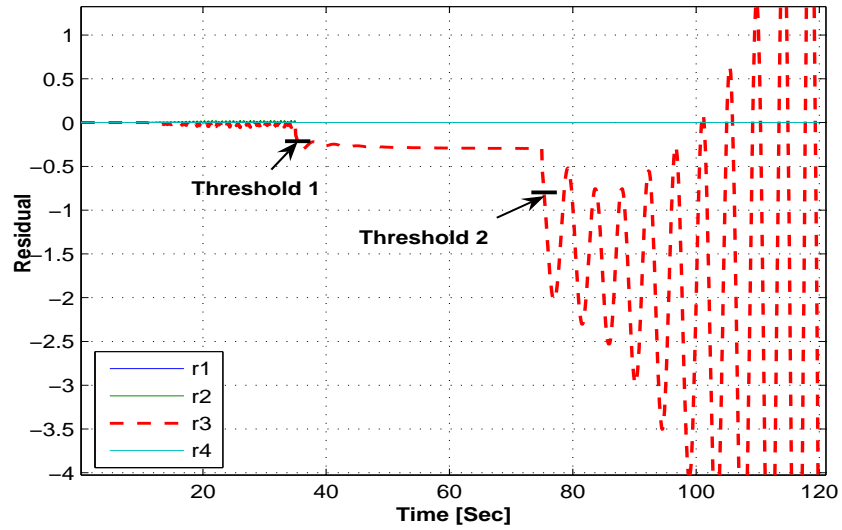


Figure 3.4: Multiple failures in single actuator Rudder 20% at 35 Secs and 80% at 75 Secs

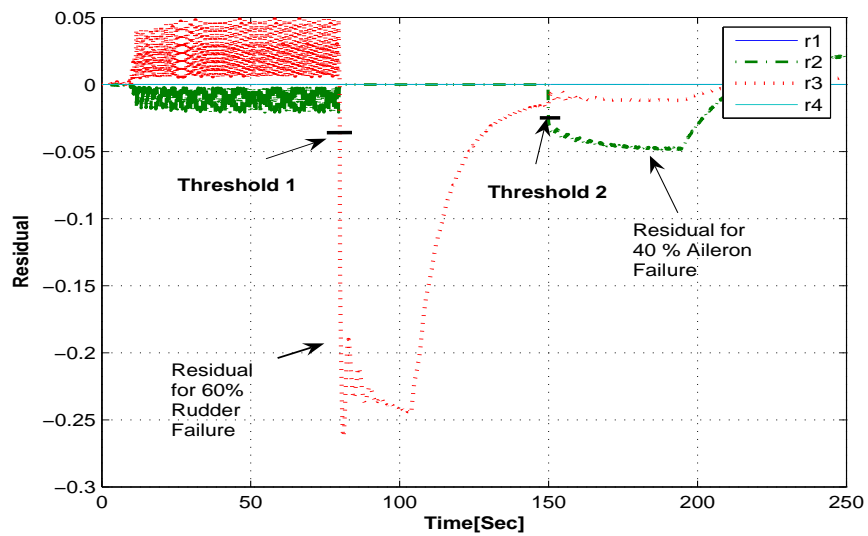


Figure 3.5: Multiple failures in different actuators 60% Rudder failure at 75 Secs and 40% Aileron failure at 150 Secs

# Chapter 4

## Robust Fault Tolerant Control

The main component in a fault tolerant control mechanism is the design of a control system that can guarantee a minimum degree of stability of an aircraft system with faults. There are many methods in the literature, that address this design problem. In this chapter, we provide both passive and active methods for FTC design. The Linear Quadratic Regulator (LQR) and Algebraic Riccati Equation (ARE) approaches for robust control system design forms the launching point for our methods in this chapter. Most of the results in this chapter are published in [41].

**Definition 4.1. *Nominal Controller:*** *A controller designed to guarantee stability and performance without considering faults or uncertainties i.e., controllers designed for a nominal model (2.5).*

**Definition 4.2. *Robust FTC:*** *A controller that guarantee stability and performance of closed loop system with a faulty (3.1) and (or) an uncertain system (2.15).*

### 4.1 LQR Based Nominal Controller Design

In this section we consider the design of nominal controller. By our practical assumption 3.1 we have all the measurements of states which enable us to design a state feedback controller using LQR and ARE theory. For convenience, here, we describe a nominal model in state space

$$\dot{x}(t) = Ax(t) + Bu(t), \quad x(0) = x_0. \quad (4.1)$$

**Assumption 4.1.** *(A, B) is stabilizable.*

Without Assumption 4.1 the design of either nominal or fault tolerant controller is not possible.

The nominal optimal state feedback controller denoted as  $K_n$  is designed for nominal model 4.1 to guarantee closed loop stability and to achieve the given performance specifications. In this thesis, the controller  $K_n$  is chosen to minimize the quadratic cost function

$$J = \int_0^{\infty} (x^T Q x + u^T R u) dt \quad (4.2)$$

where  $Q = Q^T \geq 0$ ,  $R = R^T > 0$  are weighting matrices that serve as design parameters in constraining system states and control input.

To facilitate the following presentation, we shall further make the following assumptions.

**Assumption 4.2.**  $R$  is a diagonal matrix;  $R = \text{diag}[r_1, \dots, r_m] > 0$  and,

**Assumption 4.3.**  $(Q, A)$  is detectable.

Even though these assumptions are fairly standard in practice, we want to emphasize that diagonal structure of  $R$  is critical to the following development and it does not seem that it can be relaxed.

Optimal state feedback controller  $K_n$  can be obtained by finding the real symmetric stabilizing solution  $X = X^T \geq 0$  to the following algebraic Riccati equation (ARE)

$$A^T X + X A - X B R^{-1} B^T X + Q = 0. \quad (4.3)$$

The optimal state feedback controller is given by

$$K_n = -R^{-1} B^T X \quad (4.4)$$

and the closed-loop system

$$\dot{x}(t) = (A + B K_n) x(t) \quad (4.5)$$

is asymptotically stable and the optimal cost function is given by

$$J = x^T(0) X x(0), \quad \forall x(0) \neq 0. \quad (4.6)$$

See [1] for more details on LQR theory.

## 4.2 Robust Control Reconfiguration

When fault is detected by the FDI mechanism a pre-defined controller reconfiguration or switching mechanism is initiated with a switching signal  $s(t)$ . A switching logic based on threshold levels initiates switching signal  $s(t)$  in order to maintain both closed loop stability and performance see [17, 21].

A simple switching logic to construct switching signal  $s(t)$  is mentioned below

$$\begin{aligned} \text{If } \|r_1(f, t)\| > T_{1f}, \text{ Then } K = K_f \\ \text{else } K = K_n. \end{aligned}$$

The block diagram for multiple controllers switching based reconfiguration with an integrator in the outer-loop for tracking is shown in Figure 4.1.

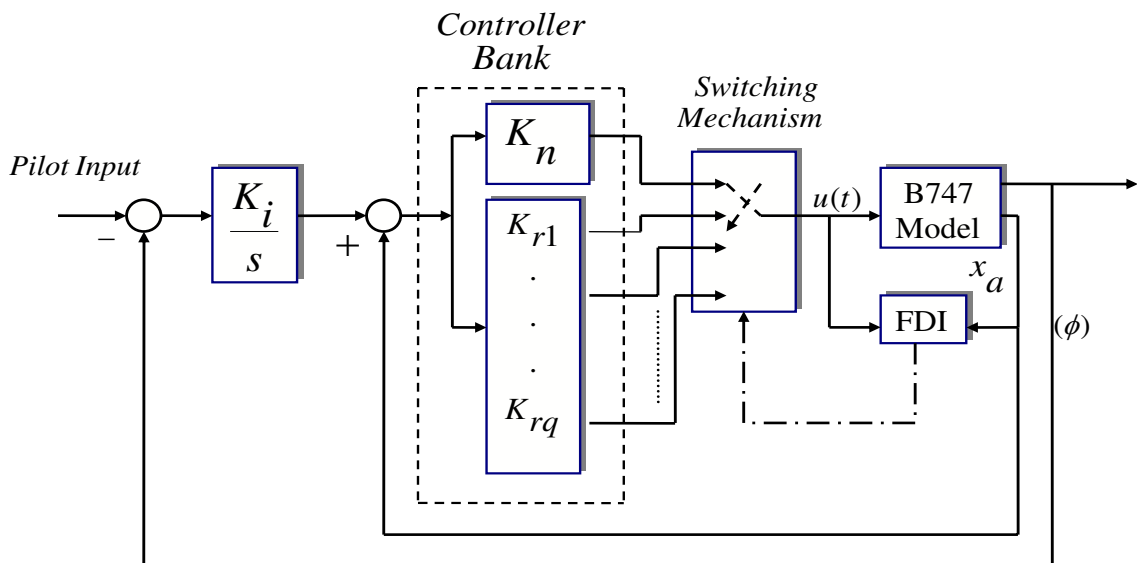


Figure 4.1: Reconfiguration mechanism with bank of controllers

### 4.2.1 Optimal Robust Controller Design under Actuator Faults

This subsection presents a new way of designing optimal controllers which are robust and optimal to actuator faults. We start by considering failure in one actuator and later we generalize the design procedure to multiple actuator failures and system with polytopic uncertainties.

As mentioned earlier, actuator failure resulting in loss of efficiency in the control effort is considered in this thesis. The faulty  $B$  matrix encapsulating loss of gain in a single actuator channel is given by  $\hat{B}_i = B(I - e_i e_i^T \varepsilon_i)$ .

The following lemma is a simple manipulation of the quadratic cost function (4.2) and will play a key role to our development in this thesis.

**Lemma 2.** [41] *Let  $u = K_{ri}x$  be a robust state feedback controller such that*

$$\dot{x} = (A + \hat{B}_i K_{ri})x, \quad x(0) = x_0 \quad (4.7)$$

*is stable for all  $\varepsilon_i \in [0, \varepsilon_{imax}]$ . Let  $\hat{X} \geq 0$  be any solution to*

$$\hat{X}(A + \hat{B}_i K_{ri}) + (A + \hat{B}_i K_{ri})^T \hat{X} + Q + K_{ri}^T R K_{ri} \leq 0. \quad (4.8)$$

*Then*

$$J(\varepsilon_i) \leq x^T(0) \hat{X} x(0) \quad (4.9)$$

*Proof.* Using the inequality (4.8), the cost function (4.2) under the  $i^{th}$  actuator failure can be written as

$$\begin{aligned} J(\varepsilon_i) &= \int_0^\infty x^T (Q + K_{ri}^T R K_{ri}) x dt \\ &\leq - \int_0^\infty x^T [\hat{X}(A + \hat{B}_i K_{ri}) + (A + \hat{B}_i K_{ri})^T \hat{X}] x dt \\ &= - \int_0^\infty (x^T \hat{X} \dot{x} + \dot{x}^T \hat{X} x) dt \\ &= - \int_0^\infty \frac{d}{dt} x^T \hat{X} x dt \\ &= x^T(0) \hat{X} x(0) - x^T(\infty) \hat{X} x(\infty) \\ &= x^T(0) \hat{X} x(0) \end{aligned}$$

since the system is stable and  $x(\infty) = 0$ . □

In the following, we shall propose a new technique to design the optimal robust state feedback controller  $K_{ri}$  so as to guarantee both closed-loop stability and performance for all stages of the  $i^{th}$  actuator fault.

The following theorem shows that the optimal controller designed considering this worst possible case is the desired optimal robust controller for faults of magnitude within  $\varepsilon_{imax}$ . Now we recollect  $B_{imin} = B(I - e_i e_i^T \varepsilon_{imax})$  representing the maximum or the worst possible case of failure  $\varepsilon_{imax}$  in the  $i^{th}$  actuator.

**Theorem 2.** [41] Suppose  $(A, B_{imin})$  is stabilizable and let  $X_i \geq 0$  be the stabilizing solution to the following ARE

$$X_i A + A^T X_i + Q - X_i B_{imin} R^{-1} B_{imin}^T X_i = 0. \quad (4.10)$$

Then

$$K_{ri} = -R^{-1} B_{imin}^T X_i \quad (4.11)$$

is the optimal robust controller in the sense that the closed-loop system

$$\dot{x} = (A + \hat{B}_i K_{ri})x, \quad x(0) = x_0$$

is stable for all  $\varepsilon_i \in [0, \varepsilon_{imax}]$  and the following worst case cost function is minimized

$$\min_{K_{ri}} \max_{\varepsilon_i \in [0, \varepsilon_{imax}]} J(\varepsilon_i) = x^T(0) X_i x(0). \quad (4.12)$$

*Proof.* First of all, it is clear that

$$\begin{aligned} \min_{K_{ri}} \max_{\varepsilon_i \in [0, \varepsilon_{imax}]} J(\varepsilon_i) &\geq \min_{K_{ri}} J(\varepsilon_{imax}) \\ &= x^T(0) X_i x(0). \end{aligned}$$

To complete the proof, by applying Lemma 2, we only need to show that  $A + \hat{B}_i K_{ri}$  is stable for all  $\varepsilon_i \in [0, \varepsilon_{imax}]$  and

$$X_i(A + \hat{B}_i K_{ri}) + (A + \hat{B}_i K_{ri})^T X_i + Q + K_{ri}^T R K_{ri} \leq 0 \quad (4.13)$$

for all  $\varepsilon_i \in [0, \varepsilon_{imax}]$ .

Since  $\varepsilon_i$  appears linearly in the inequality (4.13), this inequality holds for all  $\varepsilon_i$  if and only if it holds at the two extreme points:

1. *No-fault situation:*

$$X_i(A + B K_{ri}) + (A + B K_{ri})^T X_i + Q + K_{ri}^T R K_{ri} \leq 0 \quad (4.14)$$

2. *Maximum fault situation:*

$$X_i(A + B_{imin} K_{ri}) + (A + B_{imin} K_{ri})^T X_i + Q + K_{ri}^T R K_{ri} \leq 0. \quad (4.15)$$

It is easy to verify that the left hand side of (4.15) is exactly the same as that of (4.10) and hence the inequality is satisfied.

Substituting  $K_{ri}$  from (4.11) into the left hand side of (4.14) and using the equation (4.10), we get

$$X_i A + A^T X_i + Q - X_i B R^{-1} B_{imin}^T X_i - X_i B_{imin} R^{-1} B^T X_i + X_i B_{imin} R^{-1} B_{imin}^T X_i$$

$$\begin{aligned}
&= 2X_i B_{imin} R^{-1} B_{imin}^T X_i - X_i B R^{-1} B_{imin}^T X_i - X_i B_{imin} R^{-1} B^T X_i \\
&= 2X_i B_{imin} R^{-1} B_{imin}^T X_i - X_i (B_{imin} + B e_i e_i^T \varepsilon_{imax}) R^{-1} B_{imin}^T X_i \\
&\quad - X_i B_{imin} R^{-1} (B_{imin} + B e_i e_i^T \varepsilon_{imax})^T X_i \\
&= -X_i B e_i e_i^T \varepsilon_{imax} R^{-1} B_{imin}^T X_i - X_i B_{imin} R^{-1} e_i e_i^T B^T X_i \varepsilon_{imax} \\
&= -\varepsilon_{imax} X_i B (e_i e_i^T R^{-1} (I - e_i e_i^T \varepsilon_{imax}) + (I - e_i e_i^T \varepsilon_{imax}) R^{-1} e_i e_i^T) B^T X_i \\
&= -\varepsilon_{imax} X_i B \begin{bmatrix} 0 & \cdots & \cdots & \cdots & 0 \\ \vdots & \ddots & & & \vdots \\ \vdots & & \frac{2(1-\varepsilon_{imax})}{r_i} & & \vdots \\ \vdots & & & \ddots & \vdots \\ 0 & \cdots & \cdots & \cdots & 0 \end{bmatrix} B^T X_i \leq 0.
\end{aligned}$$

Hence inequality (4.13) holds for all fault intensities in  $i^{th}$  actuator ( $\forall \varepsilon_i \in [0, \varepsilon_{imax}]$ ). Note that it is critical for  $R$  to be diagonal in the last inequality.

Now to show that the closed loop  $(A + \hat{B}_i K_{r_i})$  is stable for all  $\varepsilon_i \in [0, \varepsilon_{imax}]$  we proceed by a contradiction. Assume  $A + \hat{B}_i K_{r_i}$  is not stable for some  $\varepsilon_i \in [0, \varepsilon_{imax}]$ , i.e., there is a  $\lambda$  with  $Re\lambda \geq 0$  and a vector such that

$$(A + \hat{B}_i K_{r_i})x = \lambda x.$$

Pre-multiplying and post-multiplying inequality (4.13) by  $x^T$  and  $x$ , we get

$$2Re\lambda(x^T X_i x) + x^T Q x + x^T K_{r_i}^T R K_{r_i} x \leq 0$$

Since  $Re\lambda \geq 0$ , we have  $Qx = 0$ ,  $K_{r_i} x = 0$ .

This in turn implies

$$(A + \hat{B}_i K_{r_i})x = Ax = \lambda x,$$

i.e.,  $(Q, A)$  is not detectable.

This is a contradiction to Assumption 4.3. Hence  $A + \hat{B}_i K_{r_i}$  must be stable for all  $\varepsilon_i \in [0, \varepsilon_{imax}]$ .  $\square$

We have so far described the design of robust controllers for a single actuator fault. It is quite possible in an aircraft system that more than one actuator can fail at the same time or one after another. It is therefore of paramount importance to be able to handle multiple actuator failures when they occur. Nevertheless, it is not hard to extend the above design scheme to handle multiple actuator faults.

Let  $\mathcal{K}$  represent a faulty set of  $k$  actuator failures occurring simultaneously. Now recalling the definitions of fault modelling for multiple faults described as

$$B_{min} = B \left( I - \sum_{i \in \mathcal{K}} e_i e_i^T \varepsilon_{imax} \right) \quad (4.16)$$

and

$$\hat{B} = B(I - \sum_{i \in \mathcal{K}} e_i e_i^T \varepsilon_i), \quad \hat{B} = B \prod_{i \in \mathcal{K}} (I - e_i e_i^T \varepsilon_i).$$

**Theorem 3.** [41] Suppose  $(A, B_{min})$  is stabilizable and let  $X_{min} \geq 0$  be the stabilizing solution to the following ARE

$$X_{min}A + A^T X_{min} + Q - X_{min}B_{min}R^{-1}B_{min}^T X_{min} = 0 \quad (4.17)$$

Then

$$K_r = -R^{-1}B_{min}^T X_{min} \quad (4.18)$$

is the optimal robust controller in the sense that the closed-loop system

$$\dot{x} = (A + \hat{B}K_r)x, \quad x(0) = x_0$$

is stable for all  $\varepsilon_i \in [0, \varepsilon_{imax}]$ ,  $i \in \mathcal{K}$  and the following worst case cost function for  $k$  actuator failures is minimized

$$\min_{K_r} \max_{i \in \mathcal{K}, \varepsilon_i \in [0, \varepsilon_{imax}]} J(\varepsilon_i, \forall i \in \mathcal{K}) = x^T(0)X_{min}x(0).$$

*Proof.* The proof of this theorem is very similar to the proof of Theorem 2. First of all, it is clear that

$$\begin{aligned} \min_{K_r} \max_{i \in \mathcal{K}, \varepsilon_i \in [0, \varepsilon_{imax}]} J(\varepsilon_i, \forall i \in \mathcal{K}) &\geq \min_{K_r} J(\varepsilon_i = \varepsilon_{imax}, \forall i \in \mathcal{K}) \\ &= x^T(0)X_{min}x(0). \end{aligned}$$

To complete the proof, by Lemma 2, we only need to show that  $A + \hat{B}K_r$  is stable for all  $\varepsilon_i \in [0, \varepsilon_{imax}]$ ,  $\forall i \in \mathcal{K}$  and

$$X_{min}(A + \hat{B}K_r) + (A + \hat{B}K_r)^T X_{min} + Q + K_r^T R K_r \leq 0$$

for all  $\varepsilon_i \in [0, \varepsilon_{imax}]$ ,  $\forall i \in \mathcal{K}$ .

Substituting  $K_r$  from (4.18) into the left hand side of the above inequality and using the equation (4.17), we get

$$\begin{aligned} &X_{min}A + A^T X_{min} + Q - X_{min}\hat{B}R^{-1}B_{min}^T X_{min} - X_{min}B_{min}R^{-1}\hat{B}^T X_{min} \\ &\quad + X_{min}B_{min}R^{-1}B_{min}^T X_{min} \\ = &2X_{min}B_{min}R^{-1}B_{min}^T X_{min} - X_{min}\hat{B}R^{-1}B_{min}^T X_{min} - X_{min}B_{min}R^{-1}\hat{B}^T X_{min} \\ = &-X_{min}B \sum_{i \in \mathcal{K}} e_i e_i^T (\varepsilon_{imax} - \varepsilon_i) R^{-1} B_{min}^T X_{min} \\ &\quad - X_{min}B_{min}R^{-1} \sum_{i \in \mathcal{K}} e_i e_i^T (\varepsilon_{max} - \varepsilon_i) B^T X_{min} \\ = &-2X_{min}B \sum_{i \in \mathcal{K}} e_i e_i^T (\varepsilon_{imax} - \varepsilon_i) / r_i (I - \sum_{i \in \mathcal{K}} e_i e_i^T \varepsilon_{imax}) B^T X_{min} \\ = &-2X_{min}B \sum_{i \in \mathcal{K}} \prod_{j \in \mathcal{K}} (\varepsilon_{imax} - \varepsilon_j) / r_i e_i e_i^T (1 - \varepsilon_{jmax} e_j e_j^T) B^T X_{min} \leq 0. \end{aligned}$$

The proof for stability of the closed-loop system is the same as in Theorem 2.  $\square$

## 4.2.2 Optimal Robust Control with Model Uncertainty and Actuator Failures

The robust control design with both single and multiple actuator failures discussed so far assumes that the system model is perfectly accurate. This of course is not very realistic in practical applications. We shall now extend the above results to some classes of systems with possibly both model uncertainties and actuator failures.

We shall assume that the model uncertainties on the  $A$  matrix can be approximately described by a convex hull of a set of vertex matrices.

**Theorem 4.** [41] Suppose  $A \in \mathcal{A} = \text{Co}[A_1, A_2 \dots A_l]$  and define  $B_{min} = B(I - \sum_{i \in \mathcal{K}} e_i e_i^T \varepsilon_{imax})$ . Suppose  $(A_i, B_{min})$  is stabilizable and  $(Q, A_i)$  is detectable for all  $i = 1, \dots, l$ . Let  $X_{min} \geq 0$  satisfy simultaneously the following inequality

$$X_{min}A_i + A_i^T X_{min} + Q - X_{min}B_{min}R^{-1}B_{min}^T X_{min} \leq 0, \quad i = 1, \dots, l. \quad (4.19)$$

Then

$$K_r = -R^{-1}B_{min}^T X_{min}$$

stabilizes

$$\dot{x} = (A + \hat{B}K_r)x, \quad x(0) = x_0, \quad A \in \mathcal{A}$$

for all  $\varepsilon_i \in [0, \varepsilon_{imax}]$ ,  $\forall i \in \mathcal{K}$  and

$$\min_{K_r} \max_{A \in \mathcal{A}} \max_{i \in \mathcal{K}, \varepsilon_i \in [0, \varepsilon_{imax}]} J(\varepsilon_i, \forall i \in \mathcal{K}) \leq x^T(0)X_{min}x(0).$$

*Proof.* This follows from Theorem 3 if

$$X_{min}A + A^T X_{min} + Q - X_{min}B_{min}R^{-1}B_{min}^T X_{min} \leq 0,$$

for all  $A \in \mathcal{A}$ . Since  $\mathcal{A}$  is a convex hull of a set of vertex matrices, the above inequality holds for all  $A \in \mathcal{A}$  if and only if it holds on the vertices [9], i.e.,

$$X_{min}A_i + A_i^T X_{min} + Q - X_{min}B_{min}R^{-1}B_{min}^T X_{min} \leq 0, \quad i = 1, \dots, l.$$

□

It is usually rather hard to solve the set of ARE inequalities in the above theorem. However, the set of ARE inequalities can be converted into a set of linear matrix inequalities (LMIs) under some minor restrictions on  $Q$ .

**Corollary 1.** Assume in Theorem 4 that  $(Q, A_i)$  is observable and  $X_{min} \geq 0$  satisfying inequality (4.19), then  $X_{min} > 0$ . Furthermore, let  $Y_m = X_{min}^{-1}$ , then  $Y_{min}$  satisfies

$$\begin{bmatrix} A_i Y_m + Y_m A_i^T - B_{min} R^{-1} B_{min}^T & Y_m Q^{\frac{1}{2}} \\ Q^{\frac{1}{2}} Y_m & -I \end{bmatrix} \leq 0, \quad i = 1, \dots, l. \quad (4.20)$$

*Proof.* Suppose  $X_{min} \geq 0$  is singular and let  $0 \neq x \in \mathbb{R}^n$  be such that  $X_{min}x = 0$ , i.e.,  $x \in \text{Ker}(X)$ . Multiply inequality (4.19) from right by  $x$  and from left by  $x^T$ , we get  $x^T Q x = 0$ . Hence  $Qx = 0$  since  $Q \geq 0$ . Now multiply inequality (4.19) from right by  $x$ , we get  $X_{min}A_i x = 0$ . Hence  $\text{Ker}(X_{min})$  is a  $A_i$ -invariant subspace and it is therefore possible to choose  $x$  such that it is an eigenvector of  $A_i$  corresponding to some eigenvalue  $\lambda$ , i.e.,  $A_i x_i = \lambda x_i$ . By Popov-Belevitch-Hautus (PBH) test [40], we can conclude that  $(Q, A_i)$  is not observable, which is a contradiction. Hence  $X_{min}$  must be nonsingular. Now it is straightforward to convert the inequality (4.19) into the LMI (4.20) by letting  $Y_m = X_{min}^{-1}$ .  $\square$

### 4.2.3 Application of AFTC for Linear Boeing 747 Model

In this subsection we will employ the nominal and robust controller design methodologies mentioned earlier subsections to control a linear B747 aircraft model. The simulation is conducted on a linear considering multiple fault percentages in single and multiple actuators. The FDI mentioned in Sub-Section 3.3.3 initiates a switching signal after the residual signal  $r_i(t)$  exceeds a certain threshold level for  $i^{th}$  actuator. Figure 4.2 demonstrates that the robust optimal controller designed considering 80% rudder failure guarantees both performance and stability whereas, nominal controller fails to guarantee stability for 80% Rudder failure. Similarly Figure 4.3 depicts controller reconfiguration to worst-case controller of the corresponding actuators (Aileron and Rudder) retains the stability and performance of the closed loop system.

**Remark 4.1.** *Once the controller is reconfigured to a worst-case controller it remains in the loop for the whole flight operation until a reset mechanism is implemented after corrective action is taken to fix the actuator fault.*

## 4.3 Passive FTC

For the completeness in the discussion of FTC methodologies, in this section we discuss Passive FTC (PFTC) also known as reliable control method. In PFTC, a worst case faulty case is assumed and controller is designed for the assumed fault. There is no controller reconfiguration employed in PFTC method and this may result design of very conservative controllers. There is lot attention drawn towards the design of reliable controller in the literature. Recent work in the design of reliable controllers and their application for aircraft systems can be seen in [20, 36].

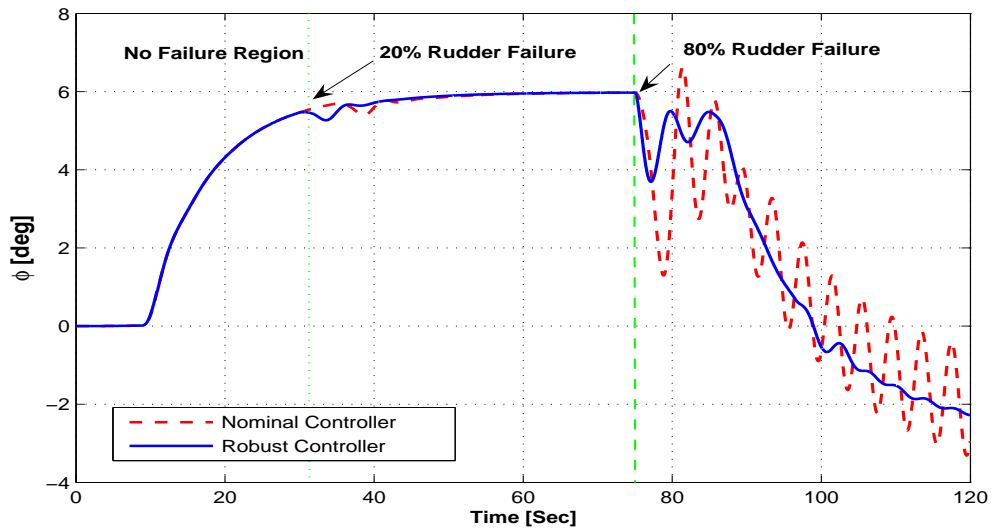


Figure 4.2: Roll angle ( $\phi$ ) response with both Nominal Controller (*dashed*) and Robust Controller (*solid*) for Rudder failure of different fault intensities

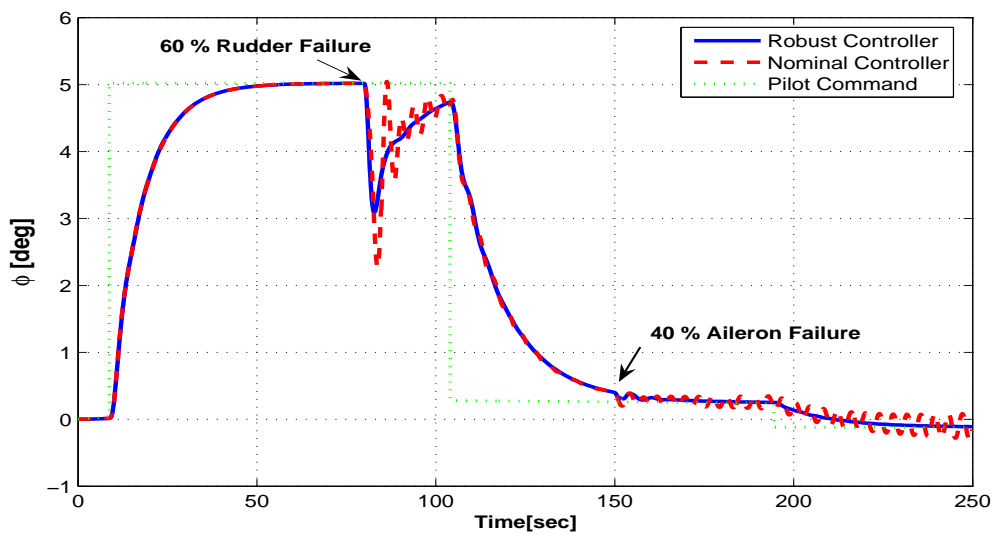


Figure 4.3: Roll angle response with nominal controller (*dashed*) and Robust controller (*solid*) with 60% Rudder failure at 80 seconds and 40% Aileron failure at 150 seconds

### 4.3.1 Reliable Controller Design

The nominal dynamic system with norm-bounded uncertainties is defined by:

$$\dot{x}(t) = (A_0 + E_1\Delta_1F_1)x(t) + (B_0 + E_2\Delta_2F_2)u(t) \quad (4.21)$$

or equivalently

$$\dot{x}(t) = \mathcal{A}x(t) + \mathcal{B}u(t) \quad (4.22)$$

where  $\mathcal{A} = (A_0 + E_1\Delta_1F_1)$ ,  $\mathcal{B} = (B_0 + E_2\Delta_2F_2)$ . The constant matrices  $E_i$  and  $F_i$  where  $i = 1, 2$  represents the structure of the uncertainty in state and input matrices.

Let  $\hat{\mathcal{B}}_i = \mathcal{B}(I - e_i e_i^T \varepsilon_i)$  and  $\mathcal{B}_{imin} = \mathcal{B}(I - e_i e_i^T \varepsilon_{imax})$  represents worst case fault in  $i^{th}$  actuator. In the next theorem we give the necessary condition for robust stability of closed loop system with both norm bounded uncertainties and actuator faults.

**Theorem 5 (Robust Stability).** *Suppose  $(\mathcal{A}, \mathcal{B}_{imin})$  is stabilizable and  $(Q, \mathcal{A})$  is observable. Then, the state feedback controller  $K_{ri}$  in the control law  $u(t) = K_{ri}x(t)$  that stabilizes the closed-loop system*

$$\dot{x}(t) = (\mathcal{A} + \hat{\mathcal{B}}_i K_{ri})x(t), \quad x(0) = x_0$$

for all faults  $\varepsilon_i \in [0, \varepsilon_{imax}]$  and  $\Delta \in \mathbf{\Delta}$  is given by

$$K_{ri} = -FY^{-1}$$

where  $Y > 0$  and  $F$  are obtained from the solution of the following linear matrix inequalities

$$\begin{bmatrix} \Theta & YF_1^T & (F_2F)^T & YQ^{\frac{1}{2}} & F^T R^{\frac{1}{2}} \\ F_1Y & -S_1 & 0 & 0 & 0 \\ F_2F & 0 & -S_2 & 0 & 0 \\ Q^{\frac{1}{2}}Y & 0 & 0 & -I & 0 \\ R^{\frac{1}{2}}F & 0 & 0 & 0 & -I \end{bmatrix} < 0, \quad (4.23)$$

$$\begin{bmatrix} \Gamma & YF_1^T & F_{2f}^T & YQ^{\frac{1}{2}} & F^T R^{\frac{1}{2}} \\ F_1Y & -S_1 & 0 & 0 & 0 \\ F_{2f} & 0 & -S_2 & 0 & 0 \\ Q^{\frac{1}{2}}Y & 0 & 0 & -I & 0 \\ R^{\frac{1}{2}}F & 0 & 0 & 0 & -I \end{bmatrix} < 0 \quad (4.24)$$

with

$$\Theta = A_0Y + YA_0^T - (B_0F) - (B_0F)^T + E_1S_1E_1^T + E_2S_2E_2^T,$$

$$\Gamma = A_0Y + YA_0^T + [B_0(e_i e_i^T \varepsilon_{imax} - I)F] + [B_0(e_i e_i^T \varepsilon_{imax} - I)F]^T + E_1S_1E_1^T + E_2S_2E_2^T$$

and  $F_{2f} = [F_2(e_i e_i^T \varepsilon_{imax} - I)F]$ .

*Proof.* Considering the ARE for system with  $i^{th}$  actuator failure and uncertainties as:

$$\begin{aligned} X(\mathcal{A} + \hat{\mathcal{B}}_i K_{ri}) + (\mathcal{A} + \hat{\mathcal{B}}_i K_{ri})^T X + Q + K_{ri}^T R K_{ri} &< 0 \\ \Rightarrow X[(A_0 + E_1 \Delta_1 F_1) + (B_0 + E_2 \Delta_2 F_2)(I - e_i e_i^T \varepsilon_i) K_{ri}] &+ [(A_0 + E_1 \Delta_1 F_1) \\ + (B_0 + E_2 \Delta_2 F_2)(I - e_i e_i^T \varepsilon_i) K_{ri}]^T X + Q + K_{ri}^T R K_{ri} &< 0. \end{aligned} \quad (4.25)$$

Expanding and collecting the terms in the above inequality we get

$$\begin{aligned} X A_0 + A_0^T X + X[B_0(I - e_i e_i^T \varepsilon_i) K_{ri}] + [B_0(I - e_i e_i^T \varepsilon_i) K_{ri}]^T X \\ + X[E_2 \Delta_2 F_2(I - e_i e_i^T \varepsilon_i) K_{ri}] + [E_2 \Delta_2 F_2(I - e_i e_i^T \varepsilon_i) K_{ri}]^T X \\ + (E_1 \Delta_1 F_1)^T X + X(E_1 \Delta_1 F_1) + Q + K_{ri}^T R K_{ri} &< 0. \end{aligned} \quad (4.26)$$

The above inequality (4.26) is linear in  $\varepsilon_i$  and it holds for all  $\varepsilon_i \in [0, \varepsilon_{imax}]$  if and only if it satisfies extreme cases  $\varepsilon_i = 0$  and  $\varepsilon_i = \varepsilon_{imax}$ .

Equation (4.26) with no-fault condition( $\varepsilon_i = 0$ ) is:

$$\begin{aligned} X A_0 + A_0^T X + X(B_0 K_{ri}) + (B_0 K_{ri})^T X + X[E_2 \Delta_2 F_2 K_{ri}] + [E_2 \Delta_2 F_2 K_{ri}]^T X \\ + (E_1 \Delta_1 F_1)^T X + X(E_1 \Delta_1 F_1) + Q + K_{ri}^T R K_{ri} &< 0 \end{aligned} \quad (4.27)$$

and with worst case fault condition( $\varepsilon_i = \varepsilon_{imax}$ ) is:

$$\begin{aligned} X A_0 + A_0^T X + X[B_0(I - e_i e_i^T \varepsilon_{imax}) K_{ri}] + [B_0(I - e_i e_i^T \varepsilon_{imax}) K_{ri}]^T X \\ + X[E_2 \Delta_2 F_2(I - e_i e_i^T \varepsilon_{imax}) K_{ri}] + [E_2 \Delta_2 F_2(I - e_i e_i^T \varepsilon_{imax}) K_{ri}]^T X \\ + (E_1 \Delta_1 F_1)^T X + X(E_1 \Delta_1 F_1) + Q + K_{ri}^T R K_{ri} &< 0. \end{aligned} \quad (4.28)$$

Now with  $S \in \mathcal{S}$  defined in (2.8), and using Lemma 1 we can rewrite the above inequalities (4.27) and (4.28) as

$$\begin{aligned} X A_0 + A_0^T X + X(B_0 K_{ri}) + (B_0 K_{ri})^T X + X E_1 S_1 E_1^T X + F_1^T S_1^{-1} F_1 \\ + X E_2 S_2 E_2^T X + (F_2 K_{ri})^T S_2^{-1} (F_2 K_{ri}) + Q + K_{ri}^T R K_{ri} &< 0 \end{aligned} \quad (4.29)$$

and

$$\begin{aligned} X A_0 + A_0^T X + X[B_0(I - e_i e_i^T \varepsilon_{imax}) K_{ri}] + [B_0(I - e_i e_i^T \varepsilon_{imax}) K_{ri}]^T X + X E_1 S_1 E_1^T X \\ + F_1^T S_1^{-1} F_1 + X E_2 S_2 E_2^T X + [F_2(I - e_i e_i^T \varepsilon_{imax}) K_{ri}]^T S_2^{-1} [F_2(I - e_i e_i^T \varepsilon_{imax}) K_{ri}] \\ + Q + K_{ri}^T R K_{ri} &< 0. \end{aligned} \quad (4.30)$$

Pre and post multiplying (4.29) and (4.30) by  $X^{-1}$  and using change of variables *i.e.*,  $Y = X^{-1}$ ;  $Y > 0$  and  $F = -K_{ri} Y$  we get

$$\begin{aligned} A_0 Y + Y A_0^T - (B_0 F) - (B_0 F)^T + E_1 S_1 E_1^T + Y F_1^T S_1^{-1} F_1 Y \\ + (F_2 F)^T S_2^{-1} (F_2 F) + E_2 S_2 E_2^T + Y Q Y + F^T R F &< 0 \end{aligned} \quad (4.31)$$

and

$$\begin{aligned} A_0 Y + Y A_0^T + [B_0(e_i e_i^T \varepsilon_{imax} - I) F] + [B_0(e_i e_i^T \varepsilon_{imax} - I) F]^T + E_1 S_1 E_1^T \\ + Y F_1^T S_1^{-1} F_1 Y + [F_2(e_i e_i^T \varepsilon_{imax} - I) F]^T S_2^{-1} [F_2(e_i e_i^T \varepsilon_{imax} - I) F] \\ + E_2 S_2 E_2^T + Y Q Y + F^T R F &< 0. \end{aligned} \quad (4.32)$$

Applying Schur complement to inequalities (4.31) and (4.32) we obtain LMIs given as

$$\begin{bmatrix} \Theta & YF_1^T & (F_2F)^T & YQ^{\frac{1}{2}} & F^TR^{\frac{1}{2}} \\ F_1Y & -S_1 & 0 & 0 & 0 \\ F_2F & 0 & -S_2 & 0 & 0 \\ Q^{\frac{1}{2}}Y & 0 & 0 & -I & 0 \\ R^{\frac{1}{2}}F & 0 & 0 & 0 & -I \end{bmatrix} < 0, \quad (4.33)$$

$$\begin{bmatrix} \Gamma & YF_1^T & F_{2f}^T & YQ^{\frac{1}{2}} & F^TR^{\frac{1}{2}} \\ F_1Y & -S_1 & 0 & 0 & 0 \\ F_{2f} & 0 & -S_2 & 0 & 0 \\ Q^{\frac{1}{2}}Y & 0 & 0 & -I & 0 \\ R^{\frac{1}{2}}F & 0 & 0 & 0 & -I \end{bmatrix} < 0 \quad (4.34)$$

where

$$\Theta = A_0Y + YA_0^T - (B_0F) - (B_0F)^T + E_1S_1E_1^T + E_2S_2E_2^T,$$

$$\Gamma = A_0Y + YA_0^T + [B_0(e_i e_i^T \varepsilon_{imax} - I)F] + [B_0(e_i e_i^T \varepsilon_{imax} - I)F]^T + E_1S_1E_1^T + E_2S_2E_2^T$$

$$\text{and } F_{2f} = [F_2(e_i e_i^T \varepsilon_{imax} - I)F].$$

Now we show by contradiction that the robust reliable controller  $K_{ri} = -FY^{-1}$  stabilizes the closed loop  $(\mathcal{A} + \hat{\mathcal{B}}_i K_{ri})$  for all  $\varepsilon_i \in [0, \varepsilon_{imax}]$  and for all  $\Delta \in \mathbf{\Delta}$ . Let us assume  $\mathcal{A} + \hat{\mathcal{B}}_i K_{ri}$  is not stable for some  $\varepsilon_i \in [0, \varepsilon_{imax}]$  or  $\Delta \in \mathbf{\Delta}$ , i.e., there is a  $\lambda$  with  $Re\lambda \geq 0$  and a vector such that

$$(\mathcal{A} + \hat{\mathcal{B}}_i K_{ri})x = \lambda x.$$

Pre-multiplying and post-multiplying inequality (4.25) by  $x^T$  and  $x$ , we get

$$2Re\lambda(x^T X_i x) + x^T Qx + x^T K_{ri}^T R K_{ri} x < 0$$

Since  $Re\lambda \geq 0$ , we have  $Qx = 0$ ,  $K_{ri}x = 0$ .

This in turn implies

$$(\mathcal{A} + \hat{\mathcal{B}}_i K_{ri})x = \mathcal{A}x = \lambda x,$$

i.e.,  $(Q, \mathcal{A})$  is not detectable.

This is a contradiction to assumption  $(Q, \mathcal{A})$  is detectable. Hence  $\mathcal{A} + \hat{\mathcal{B}}_i K_{ri}$  must be stable for all  $\varepsilon_i \in [0, \varepsilon_{imax}]$  and  $\Delta \in \mathbf{\Delta}$ .  $\square$

In the following Example 4, we implement the proposed reliable controller design that guarantees robust stability for a linear B747 model.

**Example 4.** *The proposed method in Theorem 5 was implemented for a linear B747 model with 90% Rudder failure and structured norm bounded parameter uncertainties using YALMIP toolbox. A feasible solution was found for the set of LMIs and the closed loop  $(\mathcal{A} + \hat{\mathcal{B}}_i K_{ri})$  eigen values for the worst case is noted below. The result showing that the closed loop  $(\mathcal{A} + \hat{\mathcal{B}}_i K_{ri})$  is stable for all faults  $\varepsilon_i \in [0, 90\%]$  is depicted*

in Figure 4.4. The Matlab code for the this example is provide in Appendix B along with the simulation data.

$$e = \begin{bmatrix} -0.41 + 1.1 i \\ -0.41 - 1.1 i \\ -0.94 \\ -0.85 \\ -0.025 \\ -0.60 + 1.1 i \\ -0.60 - 1.1 i \\ -0.0017 + 0.064 i \\ -0.0017 - 0.064 i \\ -0.00026 \end{bmatrix}$$

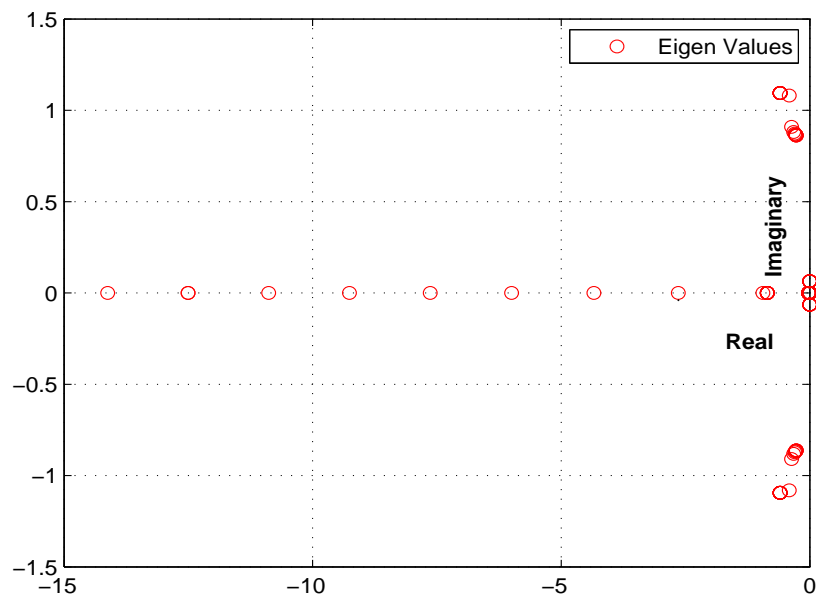


Figure 4.4: Eigen Values of  $(\mathcal{A} + \hat{\mathcal{B}}_i K_{r_i})$  for all  $\varepsilon_i \in [0, 90\%]$  of Rudder failure

From Figure 4.4, we can see that robust reliable controller  $K_{r_i}$  designed considering 90 % worst case failure in Rudder will stabilize the system for any Rudder fault with fault less than 90%.

Now in the next subsection we give a method to design a passive FTC that minimize the cost function  $J = x(0)^T Y^{-1} x(0)$ .

### 4.3.2 Guaranteed Cost Robust FTC

In aircraft systems, by Assumption 3.1 we can always measure the initial state of the system  $x(0)$ . This availability of initial state enables us to design a guaranteed cost robust fault tolerant controller. The design method of a guaranteed cost robust fault tolerant controller for the system with both actuator faults and norm bounded model uncertainties is given in next theorem.

**Theorem 6 (Guaranteed Cost).** *Suppose  $(\mathcal{A}, \mathcal{B}_{imin})$  is stabilizable. Then, the state feedback controller  $K_{ri}$  in the control law  $u = K_{ri}x$  that stabilizes the closed-loop system*

$$\dot{x} = (\mathcal{A} + \hat{\mathcal{B}}_i K_{ri})x, \quad x(0) = x_0$$

for all  $\varepsilon_i \in [0, \varepsilon_{imax}]$  and minimizes the worst case cost function

$$\min_{K_r} \max_{i \in \mathcal{K}, \varepsilon_i \in [0, \varepsilon_{imax}]} J(\varepsilon_i, \forall i \in \mathcal{K}) \leq x^T(0)Xx(0).$$

is given by

$$K_{ri} = -FY^{-1}$$

where  $Y = X^{-1}$ ,  $Y > 0$  and  $F$  are obtained from the following linear matrix inequalities

$$\min_{F, Y} \lambda \tag{4.35}$$

$$\begin{bmatrix} -\lambda & x(0)^T \\ x(0) & -Y \end{bmatrix} \leq 0 \tag{4.36}$$

and linear matrix inequalities

$$\begin{bmatrix} \Theta & YF_1^T & (F_2F)^T & YQ^{\frac{1}{2}} & F^TR^{\frac{1}{2}} \\ F_1Y & -S_1 & 0 & 0 & 0 \\ F_2F & 0 & -S_2 & 0 & 0 \\ Q^{\frac{1}{2}}Y & 0 & 0 & -I & 0 \\ R^{\frac{1}{2}}F & 0 & 0 & 0 & -I \end{bmatrix} < 0, \tag{4.37}$$

$$\begin{bmatrix} \Gamma & YF_1^T & F_{2f}^T & YQ^{\frac{1}{2}} & F^TR^{\frac{1}{2}} \\ F_1Y & -S_1 & 0 & 0 & 0 \\ F_{2f} & 0 & -S_2 & 0 & 0 \\ Q^{\frac{1}{2}}Y & 0 & 0 & -I & 0 \\ R^{\frac{1}{2}}F & 0 & 0 & 0 & -I \end{bmatrix} < 0 \tag{4.38}$$

with

$$\Theta = A_0Y + YA_0^T - (B_0F) - (B_0F)^T + E_1S_1E_1^T + E_2S_2E_2^T,$$

$$\Gamma = A_0Y + YA_0^T + [B_0(e_i e_i^T \varepsilon_{imax} - I)F] + [B_0(e_i e_i^T \varepsilon_{imax} - I)F]^T + E_1S_1E_1^T + E_2S_2E_2^T$$

$$\text{and } F_{2f} = [F_2(e_i e_i^T \varepsilon_{imax} - I)F].$$

*Proof.* It follows from Schur complement that inequality (4.36) is equivalent to  $x(0)^T Y^{-1} x(0) \leq \lambda$ . From Theorem 5, we can easily prove this Theorem 6.  $\square$

Theorem 6 also guarantees that the controllers are designed to maximize the region in state space such that any initial condition  $x_0$  starting in this region will imply  $x(t) \rightarrow 0$ . The stability regions will be invariant, which means that state trajectories originating in the region may exit but will eventually return as the state converges.

# Chapter 5

## Robustness and Safety Analysis

Till now we have discussed the design and implementation of robust reconfigurable fault tolerant controllers for linear system. In this chapter, we implement the designed robust fault tolerant controllers in the nonlinear model of Boeing 747 aircraft. The application of linear controllers in nonlinear systems is practised in the control community for the past couple of decades, one such approach is gain scheduling [30, 17].

In the next section, we briefly discuss nonlinear system implementation along with two well-known stability theorems for a nonlinear systems (see [10] for more discussion on various stability notion of nonlinear systems). Later we evaluate in detail the robustness, both stability and safety, of a closed-loop nonlinear aircraft system relative to a known nominal nonlinear system trajectory using Monte Carlo based tools.

### 5.1 Nonlinear System Implementation

A continuous time nonlinear system is described as:

$$\Xi \begin{cases} \dot{x}(t) = f(x, t, u), & x(t_0) = x_0 \in \mathbb{R}^n \\ y(t) = g(x, t, u) \end{cases} \quad (5.1)$$

where  $x(t)$  is the state of the system bounded in region  $\mathcal{X} \in \mathbb{R}^n$ ,  $u(t)$  is the control input bounded in the region  $\mathcal{U} \in \mathbb{R}^n$ ,  $y(t)$  is the output of the system,  $f$  is continuously differentiable nonlinear function, and  $g$  is a continuous nonlinear function.

The nonlinear equations of motion or degrees of freedom (DoF) for Boeing 747 form the state vector which has 10 components corresponding to force  $(\dot{\alpha}, \dot{\beta}, \dot{V}_{TAS})$ , moment  $(\dot{p}, \dot{q}, \dot{r})$ , kinematic  $(\dot{\phi}, \dot{\theta}, \dot{\psi})$  and navigation  $\dot{h}_e$  equations. Refer to [24] for extensive literature on both complete, reduced nonlinear models and their benchmark setup for FDI and FTC research.

When linear controllers both nominal  $K_n$  and robust fault tolerant controller  $K_{r_i}$  are used for nonlinear aircraft system  $\Xi$  (5.1) the following questions arise:

1. ( $Q_1$ ) Is the closed-loop system  $[\Xi, K_n]$  stable with the nominal controller?
2. ( $Q_2$ ) Is the closed loop  $[\Xi, K_{r_i}]$  with robust reconfigurable controller  $K_{r_i}$  stable upon reconfiguration?
3. ( $Q_3$ ) Is the switching based reconfiguration safe enough for passengers?

### 5.1.1 Lyapunov Stability for Nonlinear System

Nonlinear system (5.1) is stable in the sense of Lyapunov with respect to the equilibrium  $x_e = 0$ , if for any  $\epsilon > 0$  and any initial time  $t_0 \geq 0$ , there exists a constant,  $\delta = \delta(\epsilon, t_0) > 0$ , such that

$$\|x(t_0)\| < \delta \Rightarrow \|x(t)\| < \epsilon, \forall t \geq t_0. \quad (5.2)$$

This stability is illustrated by Figure 5.1.

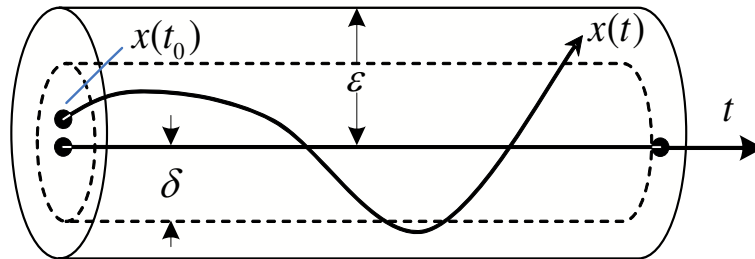


Figure 5.1: Stability in the sense of Lyapunov

### 5.1.2 Asymptotic Stability

A nonlinear system (5.1) is asymptotically stable about its equilibrium  $x_e = 0$ , if it stable in the sense of Lyapunov (5.2) and, furthermore, there exists a constant  $\delta = \delta(t_0) > 0$ , such that

$$\|x(t_0)\| < \delta \Rightarrow \|x(t)\| \rightarrow 0 \text{ as } t \rightarrow \infty. \quad (5.3)$$

**Remark 5.1.** *When a regulator is in the feedback loop, the states of the system (nonlinear and linear) are settled to a target state  $x_t$ . In which case the equilibrium state is the target state i.e.,  $x_e = x_t$ .*

## 5.2 Stability Characterization

In this section, we characterize nonlinear system stability evaluation using system state derivatives. The considered procedure is described below. First, we find  $\bar{\chi}$ , the average value of state derivative for the last 5 seconds of flight operation in the considered flight envelope.

$$\text{State derivative Avg value}(\bar{\chi}) = \frac{\sum_{i=(T-5\text{sec})/n}^{T/n} (\text{State derivative})_i}{5} \quad (5.4)$$

The nonlinear system is declared as strictly stable if  $\bar{\chi} \rightarrow 0$  for all states and is declared as stable if  $\bar{\chi} \rightarrow \epsilon$ , where  $\epsilon$  is a small neighborhood of zero (shown in Figure 5.2). The relaxed bounds  $\epsilon$  for every state is mentioned in Table 5.1.

## 5.3 Safety Certificates

In this subsection, we describe the safety conditions considered in this thesis that are used to answer question ( $Q_3$ ).

**Definition 5.1.** [28] *For nonlinear system (5.1) with the states  $x$  taking its value in  $\mathcal{X}$ , a set of initial states  $\mathcal{X}_0 \subset \mathcal{X}$ , an unsafe set  $\mathcal{X}_u \subset \mathcal{X}$ , and an safe set  $\mathcal{X}_s \subset \mathcal{X}$ . Then the safety of the system is verified, namely, there is no trajectory  $x(t)$  of the system such that  $x(0) \in \mathcal{X}_0$ ,  $x(T) \in \mathcal{X}_u$  for some  $T \geq 0$ , and  $x(t) \in \mathcal{X}_s \subset \mathcal{X}$  for all  $t \in [0, T]$ .*

Table 5.1: Stability characterization bounds

State Derivatives	Bounds
Pitch rate, $p_{body}$	$[-0.05, 0.05]$ ( $deg/s^2$ )
Roll rate, $q_{body}$	$[-0.05, 0.05]$ ( $deg/s^2$ )
Yaw rate, $r_{body}$	$[-0.05, 0.05]$ ( $deg/s^2$ )
True airspeed, $V_{TAS}$	$[-0.5, 0.5]$ ( $m/s^2$ )
Angle of Attack, $\alpha$	$[-0.05, 0.05]$ ( $deg/s^2$ )
Sideslip angle, $\beta$	$[-0.05, 0.05]$ ( $deg/s^2$ )
Pitch angle, $\theta$	$[-0.05, 0.05]$ ( $deg/s^2$ )
Roll angle, $\phi$	$[-0.05, 0.05]$ ( $deg/s^2$ )
Yaw angle, $\psi$	$[-0.05, 0.05]$ ( $deg/s^2$ )
Altitude, $h_e$	$[-10, 10]$ ( $m/s$ )

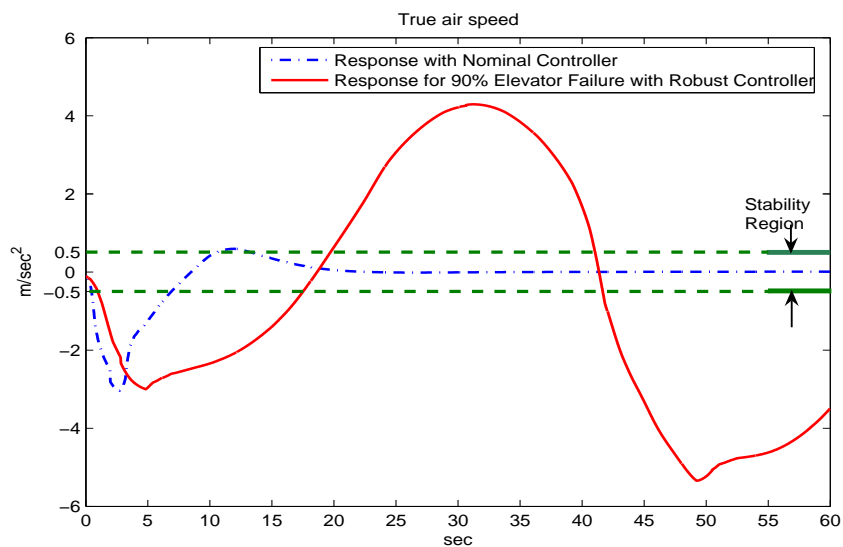


Figure 5.2: Stability region considering state derivatives

Figure 5.3 illustrates the idea of safe  $\mathcal{X}_s$  and unsafe  $\mathcal{X}_u$  sets using time responses of a nonlinear system. Other methods in the literature use convex optimization tools for safety analysis by constructing Barrier certificates (see [28] for more details). Figure 5.3 illustrates the definition of safe and unsafe regions.

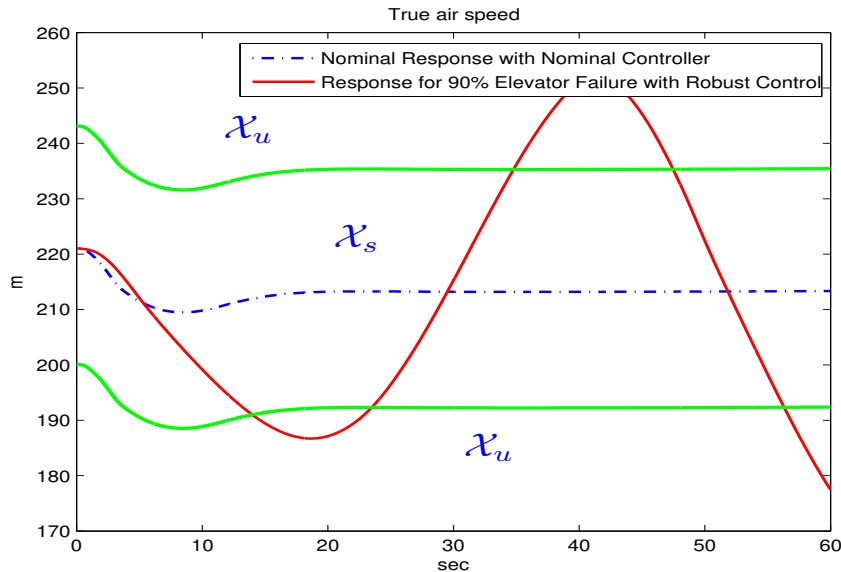


Figure 5.3: A safety certificate showing safe  $\mathcal{X}_s$  and unsafe  $\mathcal{X}_u$  regions

## 5.4 Uncertain Parameters in Switching Based Controller Reconfiguration

In this section, we define the uncertain parameters involved in the implementation of a switching based reconfigurable control in a nonlinear system. The effects of these parameters are considered in the Monte Carlo based robustness and safety analysis process.

**Definition 5.2.** *Detection and Isolation Time Delay (DITD): The minimum amount of time taken by an FDI mechanism  $T_d$  to detect and isolate a fault upon its occurrence is called DITD.  $t_d$  mainly depends on the complexity of the used FDI mechanism. DITD is illustrated in Figure 5.4.*

**Definition 5.3.** *Improper Switching: Let  $K_{r_i}$  be the controller designed for  $i^{\text{th}}$  actuator worst case failure. A switching mechanism is improper if it switches to any controller in the bank of controllers  $\mathcal{K}$  other than  $K_{r_i}$ . This is a form of controller uncertainty.*

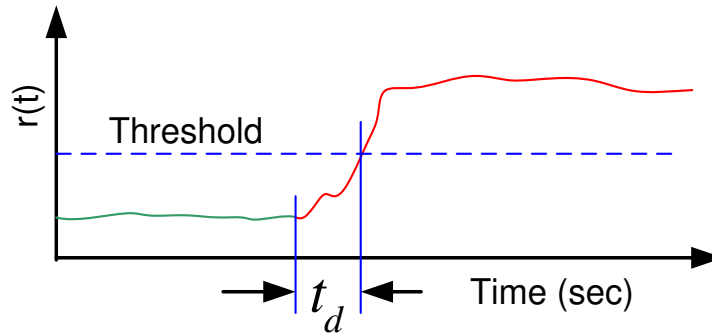


Figure 5.4: Detection time delay  $t_d$

**Assumption 5.1.** *Consecutive switching instants between robust controllers is separated by a sufficiently large time interval so that switching does not destabilize the system.*

The above assumption is general in switching control literature.

**Definition 5.4.** *Switching Delay ( $S_d$ ): The time taken or provided for a electro-mechanical switch to respond to command induced by switching logic.*

**Remark 5.2.** *Longer DITD  $t_d$  and switching delays  $S_d$  may blow off states to infinity in a short period of time i.e.,  $x(t) \rightarrow \infty$ , resulting an unstable closed loop system.*

We use probabilistic approach to analyze stability and safety in a probabilistic sense for the uncertain parameters defined in this section along with model mismatch. In the next section we give a mathematical description of probabilistic safety and stability.

## 5.5 Monte Carlo Based Robustness and Safeness Analysis

The problem at hand is to analyze the robustness of the predesigned bank of reconfigurable controllers in the presence of multiple uncertainties. Stochastic or Probabilistic methods received considerable attention lately for construction of robustness margins [4, 29, 31]. With some assumptions on uncertainty set, algorithms were developed in the literature for fast construction of robustness margin (see [12]). These methods characterize robustness of a controller by providing the measure of violation of the design requirement. The robustness evaluation integral  $\Upsilon$  is defined as the integral of the indicator function over the uncertainty sets

$$\Upsilon = \int_Q I[\Xi(q), \mathcal{K}(f)] pr(q) dq$$

where  $\Xi$  is the nonlinear aircraft model and  $q$  is the plant uncertainty state vector in the space  $Q$  with distribution  $pr(q)$ ,  $\mathcal{K}$  is the bank of controllers designed for various fault intensities  $f$ . The function  $I[\cdot]$  is a trinary indicator function and takes one of the values shown in Table 5.5.1 based on the property of the closed loop  $[\Xi(q), K_{ri}]$ , where  $K_{ri} \in \mathcal{K}, \forall i = 1, \dots, k$ .

As is well known in the robustness community that it is hard to integrate robustness integral  $\Upsilon$  of violation analytically. Monte Carlo based tools are more practical in estimating the probability and the empirical probability is calculated as

$$\hat{\Upsilon} = \frac{1}{N} \sum_{i=1}^N I[\Xi(q), \mathcal{K}(f)]$$

where  $N$  is the number of trails repeated and as  $N \rightarrow \infty$ ,  $\hat{\Upsilon} \rightarrow \Upsilon$ .

### 5.5.1 Monte Carlo Evaluation - Simulation Setup

In this subsection, we demonstrate the stability and safety analysis, using Monte Carlo simulation. We provide all the simulation conditions used in the analysis process. The fault percentages [0%, 100%] was gridded into 10 equal parts, robust controllers for each of these 10 fault percentages along with a nominal controller is designed using the methods mentioned in the last chapter. Then for every fault condition all the 11 controllers were tested simultaneously. Initial conditions for nonlinear system are randomly selected with uniform distribution. The resulting 121 combinations are tested for  $N = 50$  different initial conditions. For illustration purpose, the stability derivatives and nonlinear system states for both nominal and 90% Elevator with controller designed using 90% Elevator failure is shown in Figures 5.5 and 5.6. The robustness profile for all 121 combinations without considering switching delay  $S_d = 0$  is shown in Figure 5.7 and robustness profile with 5 secs switching delay  $S_d = 5secs$  is shown in Figure 5.8.

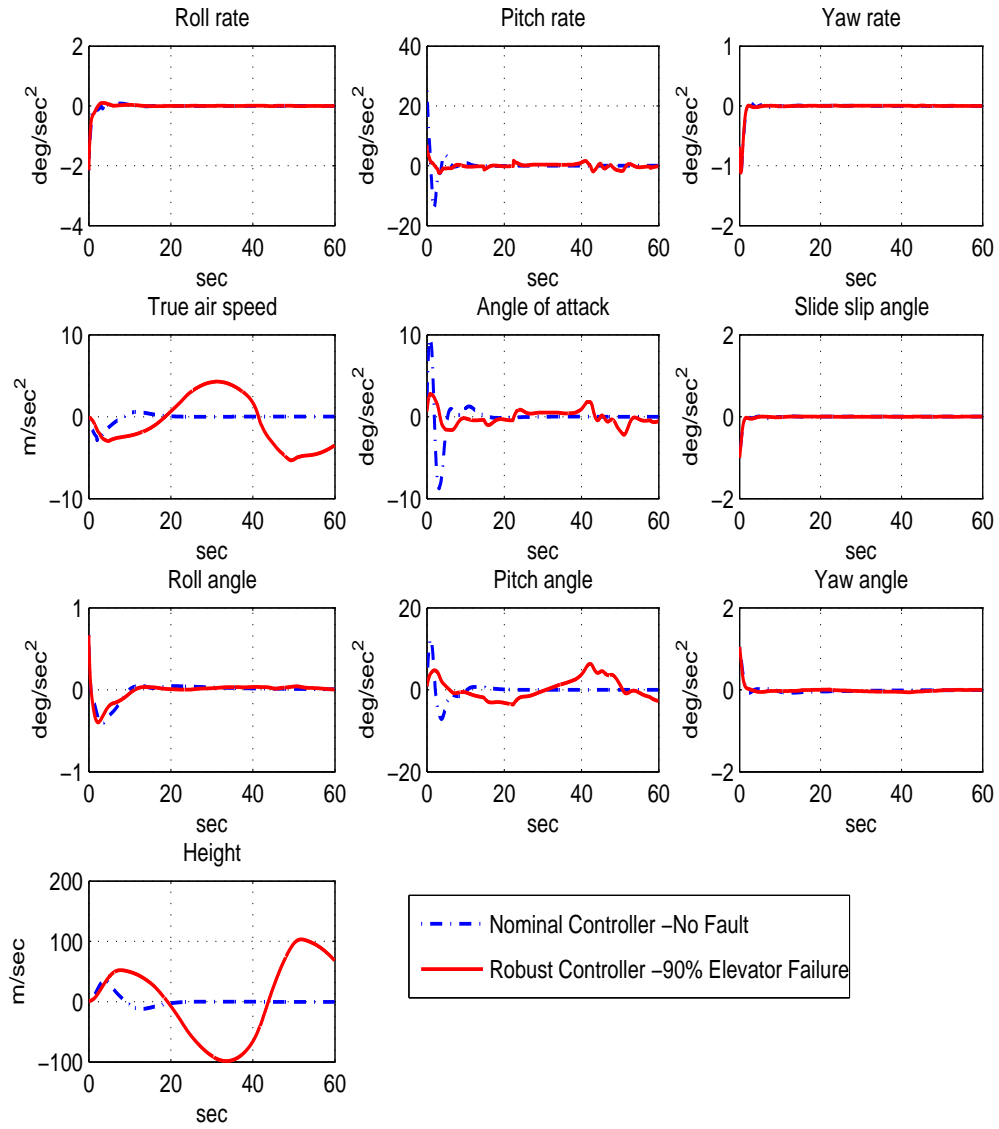


Figure 5.5: Nonlinear system stability derivatives

Table 5.2: Indicator Function

Value	Property
1	Stable and Safe
2	Stable and Unsafe
3	Unstable

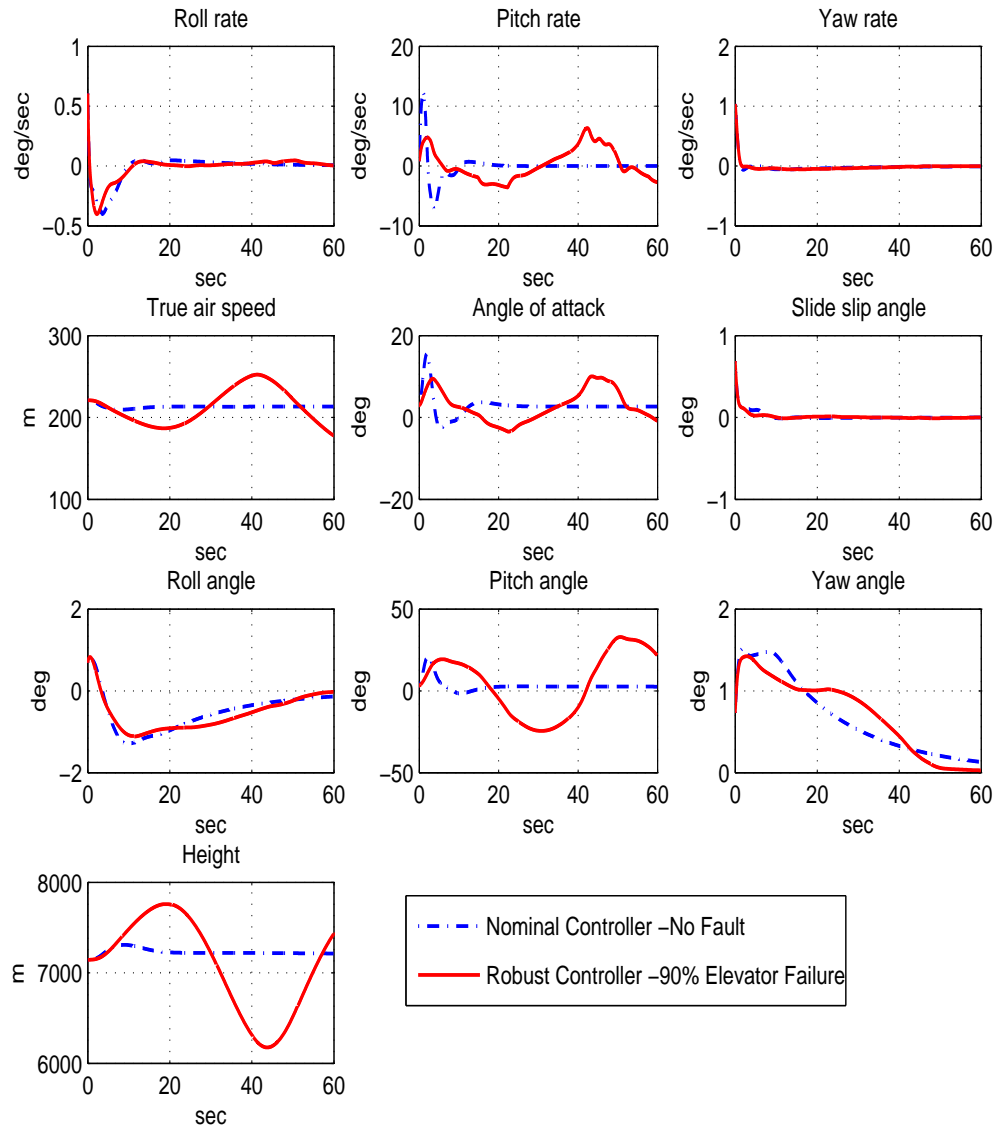


Figure 5.6: Nonlinear system states

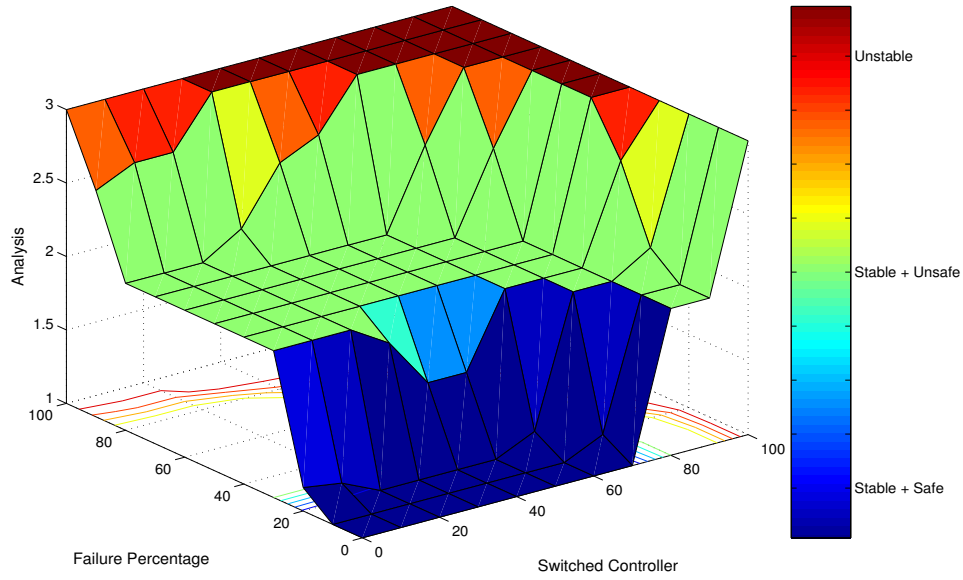


Figure 5.7: Robustness profile for Elevator with multiple controllers and no switching delay

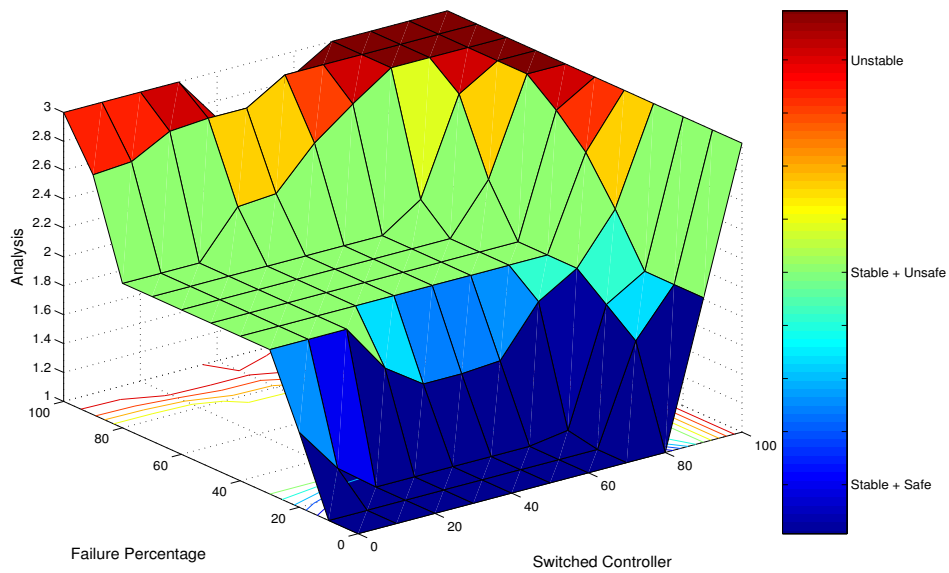


Figure 5.8: Robustness profile for Elevator with multiple controllers and 5secs switching delay

# Chapter 6

## Conclusions

The objective of this research was to design and implement fault tolerant controllers for actuator failures in Boeing 747 aircraft model. In Chapter 1 we have presented LFT based uncertainty description and provided a method for identification of a norm-bounded parameter uncertainty model of a Boeing 747 model. Chapter 2 describes fault modeling that is used in the design of fault tolerant controllers. After fault modeling in Chapter 3, we have provided Luenberger based residual generation mechanism which is used for fault detection and isolation. The effectiveness of the proposed FDI mechanism was demonstrated using simulation results on a linear B747 system. It was noticed from simulation results that by using our FDI mechanism, the fault was detected immediately after its occurrence (small detection delay).

Chapter 4 provides different methodologies of designing robust controllers that are optimal or guarantee a cost function. Our design methods rely on LQR and LMI formulation of the problem and this allows usage of various software tools to solve the problem efficiently. The knowledge about fault from FDI is used to reconfigure among the designed set of robust controllers to guarantee both stability and performance of the closed loop for both single and multiple actuator faults. In addition, in this chapter a framework for designing a reliable controller for a system with both norm-bounded parameter uncertainties and faults is mentioned.

In Chapter 5 we implemented the linear robust fault tolerant controllers in a non-linear B747 model. Monte Carlo simulation was performed and robustness and safety provided by the designed controller for different uncertainties in switching based

reconfiguration. The simulation results demonstrate, our controller design method guarantee stability criteria of the closed loop nonlinear system for all the faulty cases and safeness for most of the fault conditions.

# Bibliography

- [1] B.D.O. Anderson, J. B. Moore, *Optimal Control: Linear Quadratic Methods*, Prentice-Hall, New Jersey, 1990.
- [2] “Aviator Visual Design Simulator User Manual,” *RasSimTech LTD*, May 2003.
- [3] G. Balas, J. C. Doyle, K. Glover, A. Packard, and R. Smity,  *$\mu$ -Analysis and Synthesis Toolbox*. MUSYN Inc and The MathWorks Inc, 1994.
- [4] B. R. Barmish and C. M. Lagoa, “*The Uniform Distribution: A Rigorous Justification for Its Use in Robustness Analysis.*” *Math. Control Signals Systems*, 10 (1997), pp. 203-222.
- [5] D. Bates, I. Postlethwaite, *Robust Multivariable Control of Aerospace Systems*, Delft University Press, MG Delft, 2002.
- [6] V. Blondel and J. N. Tsitsiklis, “*NP-Hardness of Some Linear Control Design Problems,*” *SIAM J. Control Optimization*, vol. 35, pp. 2118-2127, 1997.
- [7] M. Bodson and J. E. Groszkiewicz, “*Multivariable Adaptive Algorithms for Reconfigurable Flight Control.*” *IEEE Trans. Control Systems Technology*, Vol.5, No.2, pp.217-229, 1997.
- [8] J. D. Boskovic and R. K. Mehra, “*Failure Detection, Identification and Reconfiguration in Flight Control,*” *Fault Diagnosis and Fault Tolerance for Mechatronic Systems*, Springer-verlag, New York, NY, 2002.
- [9] S. Boyd, L. El Ghaoui, E. Feron, and V. Balakrishnan, *Linear Matrix Inequalities in System and Control Theory*. SIAM , Philadelphia, PA, 1994.
- [10] G. Chen, “*Stability of Nonlinear Systems*”, (GC) book chapter, In *Wiley Encyclopedia of Electrical and Electronics Engineering*, Supplement 3, ed. by J. Webster, Wiley, New York, pp. 627-642, Feb. 2000.
- [11] J. Chen and R. J. Patton, *Robust Model-Based Fault Diagnosis for Dynamic Systems*. Kluwer Academic Publishers, Norwell, MA, 1999.
- [12] X. Chen, K. Zhou, and J. Aravena, “*Fast construction of robustness degradation function,*” *SIAM Journal on Control and Optimization*, vol. 42, pp. 1960-1971, 2004.

- [13] J. Doyle, A. Packard, K. Zhou, “*Review of LFTs, LMIs, and  $\mu$* ,” Conference on Decision and Control, pp. 1227-1232, 1991.
- [14] P.M. Frank and X. Ding, “*Survey of Robust Residual Feneration and Evaluation Methods in Observer-Based Fault Detection Systems.*” J.Proc. Cont, Vol.7, No.6, pp. 403-424, 1997.
- [15] C.Hanke, “*The Simulation of a Large Jet Transport Aircraft.*” Vol.1:Mathematical Model. Technical Report NASA CR-1756, The Boeing Company, 1971.
- [16] C.Hanke and D.Nordwall, “*The Simulation of a Jumbo Jet Transport Aircraft.*” Vol.2: Modeling Data. Technical Report NASA CR-114494/D6-30643-VOL-2, The Boeing Company,1970.
- [17] J. Hespanha, D. Liberzon, A. S. Morse, “*Overcoming the limitations of adaptive control by means of logic-based switching,*” Systems and Control Letters, Vol. 49, pp. 49-65, 2003.
- [18] S.Kanev and M.Verhaegen, “*A Bank of Reconfigurable LQG controllers for Linear System Subjected to Failures,*” Proc. CDC’00, Sydney, Australia, pp. 3684-3689, 2000.
- [19] S.Kanev, *Robust Fault Tolerant Control*, Ph.D. Thesis University of Twente, The Netherlands, 2004.
- [20] F. Liao, J.L. Wang, and G.H. Yang, “*Reliable Robust Flight Tracking Control: An LMI Appraoch*”, IEEE Trans. Control Systems Technology, Vol. 10, No. 1, pp.76-89, 2002.
- [21] D. Liberzon *Switching in Systems and Control*,Birkhauser, Boston, MA, 2003.
- [22] J. Löfberg, “YALMIP : A Toolbox for Modeling and Optimization in MATLAB”, Proceedings of the CACSD Conference, Taipei, Taiwan, 2004.
- [23] W. M. Lu, K. Zhou, J. C. Doyle, “*Stabilization of Uncertain Linear Systems: An LFT Approach,*”, IEEE Transactions on Automatic Control, Vol. 41, No. 1, pp. 50-65, 1996.
- [24] A.Marcos and G.J. Balas, “*A Boeing 747-100/200 Aircraft Fault Tolerant and Fault Diagnostic Benchmark.*” Technical report AEM-UoM-2003-1, Department of Aerospace and Engineering mechanics, University of Minnesota, USA, June, 2003.
- [25] R.J. Patton,“*Fault tolerant control: The 1997 situation (survey),*” IFAC SAFE-PROCESS’97, Hull, UK, Vol.2, pp. 1033-1055, 1997.
- [26] C. D. Persis, A. Isidori, “*A Geometric Approach to Nonlinear Fault Detection and Isolation*”, IEEE Transactions on Automatic Control, Vol. 46, No. 6, pp. 853-865, 2001.

- [27] I. R. Petersen and D. C. McFarlane, “*Optimal Guaranteed Cost Control and Filtering for Uncertain Linear Systems*,” IEEE Transactions on Automatic Control, Vol. 39, No. 9, pp. 1971-1977, 1994.
- [28] S. Prajna, A. Rantzer, “*Primal-Dual Tests for Safety and Reachability*,” In M. Morari and L. Thiele Eds *Hybrid Systems: Computation and Control*, Springer-Verlag, pp. 542-556, 2005.
- [29] L. R. Ray and R. F. Stengel, “*A monte carlo approach to the analysis of control systems robustness*,” Automatica, vol. 29, pp. 229-236, 1993.
- [30] W. J. Rugh, “*Analytical Framework for Gain Scheduling*,” IEEE Control Systems Magazine, Vol. 11, pp. 79-84, 1991.
- [31] R. F. Stengel and L. R. Ray, “*Stochastic robustness of linear time-invariant systems*,” IEEE Transaction on Automatic Control, vol. 36, pp. 82-87, 1991.
- [32] J. Stoustrup, H.Niemann, and A.la. Cour-Harbo, “*Optimal Threshold Functions for Fault Detection and Isolation*.” Proc. American Control Conference, Colorado, USA, pp. 1782-1787, 2003.
- [33] G.Tao, S. Chen, X. Tang, and S. Joshi *Adaptive Control of Systems with Actuator Failures*. Springer-Verlag, 2004.
- [34] R. M. Smith, T. A. Johansen, “*Multiple Model Approaches to Modelling and Control*,” Taylor and Francis Inc., Bristol, PA, 1997.
- [35] A. Varga, G. Looye, D. Moormann, and G. GrubelA, “*Automated Generation of LFT-Based Parametric Uncertainty*,” Mathematical and Computer Modelling of Dynamical Systems, Vol. 4, No. 4, pp. 249-274, 1998.
- [36] R. J. Veillette, J. V. Medanic, W. R.Perkins, “*Design of Reliable Control Systems*,” IEEE Trans. Autom. Control, Vol. 37, No. 3, pp. 290-304, 1992.
- [37] M. Vidyasagar, “*Randomized algorithms for robust controller synthesis using statistical learning theory*,” Automatica, vol. 37, pp. 1515-1528, 2001.
- [38] Y. M. Zhang, and J. Jiang, “*Bibliographical review on reconfigurable fault-tolerant control systems*,” Proc. of IFAC SAFEPROCESS 2003, Washington DC, U.S.A, pp 265-276, 2003.
- [39] K. Zhou, Pramod P. Khargonekar, “*Robust stabilization of linear systems with norm-bounded time-varying uncertainty*,” Systems and Control Letters, Vol. 10, No. 1, pp. 17-20, 1988.
- [40] K. Zhou, J.C. Doyle, and K. Glover, *Robust and Optimal Control*. Prentice Hall, Upper Saddle River, New Jersey, 1996.

- [41] Kemin Zhou, Phalguna K Rachinayani, Nike Liu, Zhang Ren and Jorge Aravena, "*Fault Diagnosis and Reconfigurable Control for Flight Control Systems with Actuator Failures,*" 2004 Conference on Decision and Control, Vol.5, Pg 5266 - 5271.
- [42] K. Zhou, Z. Ren, "*A New Controller Architecture for High Performance, Robust, and Fault-Tolerant Control,*" IEEE Trans. Autom. Control, Vol.46, No.10, pp. 1613-1618, 2001.

# Appendix A

## Boeing Aircraft Control Surfaces

The control surfaces are actuated by the hydraulic actuators. A hydraulic actuator used for rudder trim surface is shown in Figure A.1 and its mechanical measurements in Figure A.2. The control surfaces in Boeing 747 are described in Table A.

Figure A.3 shows the function of different actuators in an aircraft system and Figure A.4 shows the control surfaces in Boeing 747 aircraft.



Figure A.1: Linear Actuator 658D100 for Rudder trim surface (Eaton Corporation)

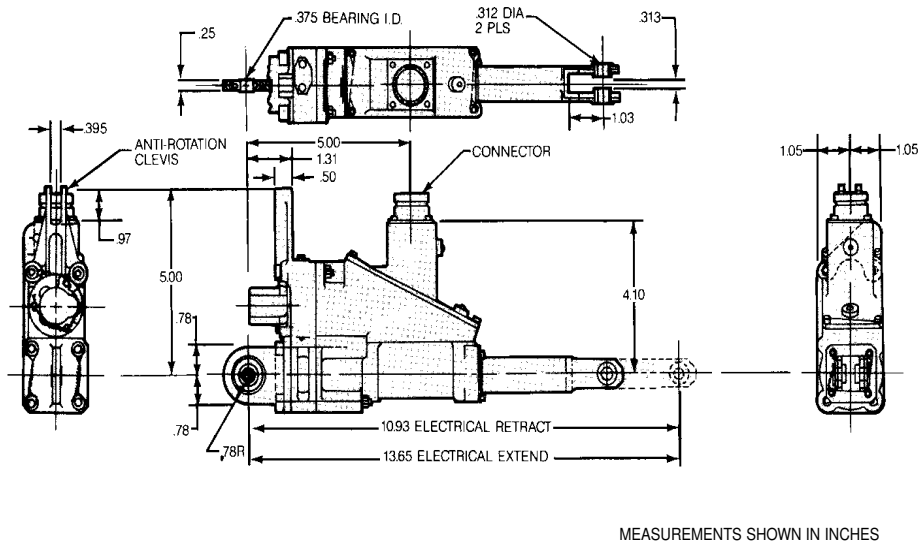


Figure A.2: Measurements of Linear Actuator 658D100 for Rudder trim surface (Eaton Corporation)

Table A.1: Boeing 747 Control Surfaces Saturation Limits

Control Surface	Maximum Deflection
Elevators	-23, +17 degrees
Horizontal Stabilizer	-12, +3 degrees
Inboard Ailerons	-20, +20 degrees
Outboard Ailerons	-25, +15 degrees
Spoilers 1,2,3,4,9,10,11,12	0, 25 degrees
Spoilers 5, 8	0, 20 degrees
Spoilers 6,7 (only speedbrakes)	0, 20 degrees
Rudder	-25, +25 degrees

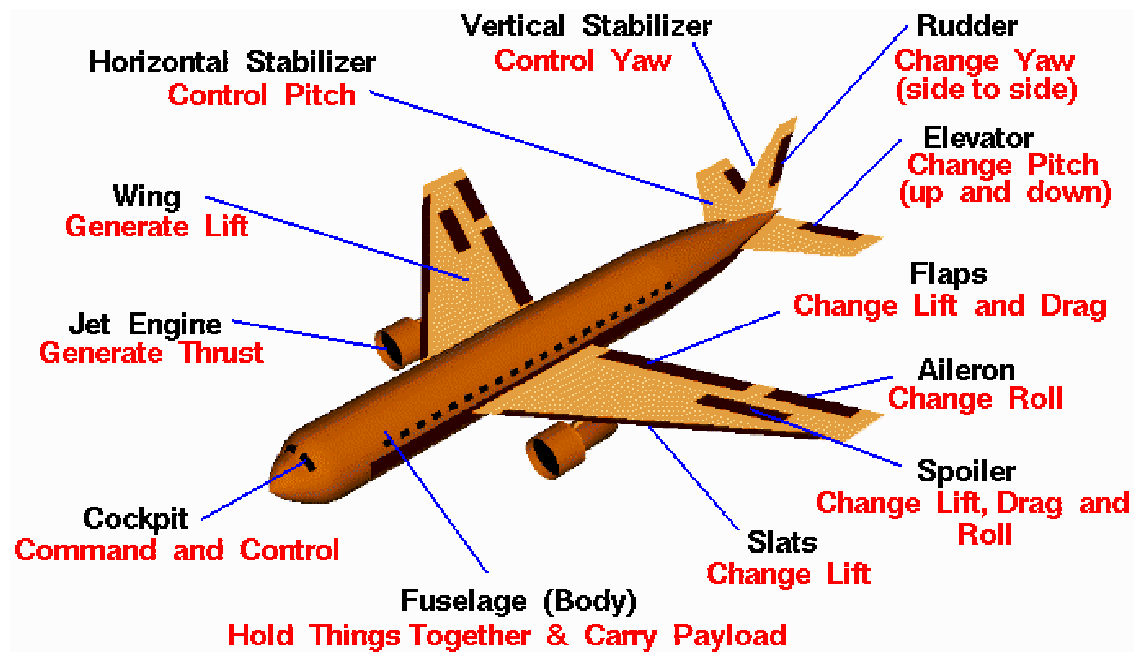


Figure A.3: Airplane actuators definition and function (NASA Glenn Research Center website)

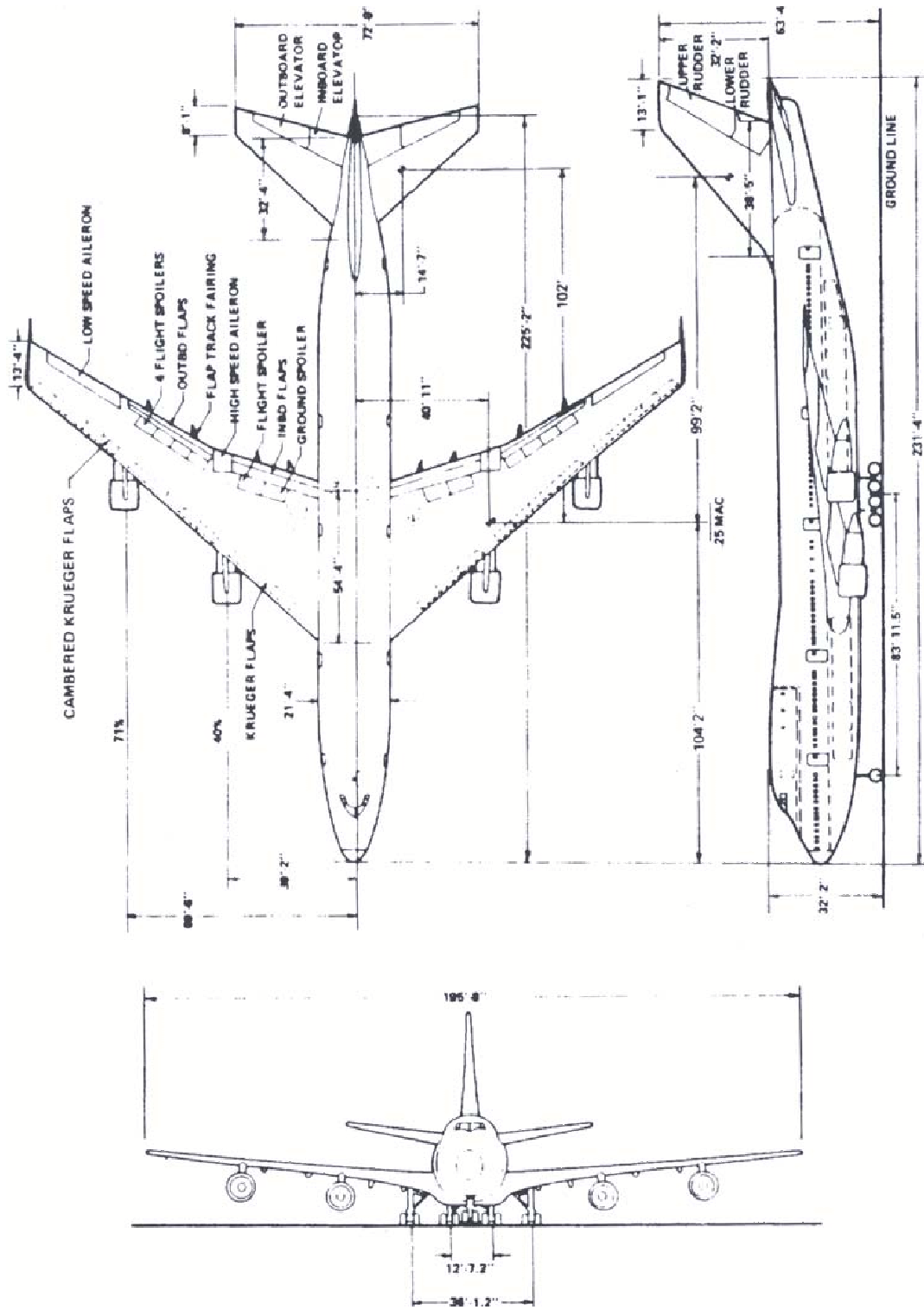


Figure A.4: Boeing 747 Three View [15]

# Appendix B

## B747 Norm Bounded Description

In this appendix we provide a norm bounded parameter uncertainty description of Boeing 747 model of the form

$$\dot{x}(t) = (A_0 + E_1\Delta_1F_1)x(t) + (B_0 + E_2\Delta_2F_2)u(t). \quad (\text{B.1})$$

The aircraft is trimmed to a straight and level flight path with parameters true air speed  $V_{TAS} \in [230m/sec, 245m/sec]$ , flight path angle  $\gamma \in [-10deg, +10deg]$  and height  $h \in [6000m, 10000m]$  and the flight path for this parameter variation set is shown in Figure 2.3.

$$A_0 = \begin{pmatrix} -0.79962 & 0 & 0.31731 & 0 & 0 & -3.2597 & 0 & 0 & 0 & 0 \\ 0 & -0.69185 & 0 & -7.7746 \times 10^{-6} & -1.2034 & 0 & 0 & 0 & 0 & 0 \\ -0.024198 & 0 & -0.15071 & 0 & 0 & 1.1682 & -0.0020 & 0 & 0 & 0 \\ 0 & -0.081745 & 0 & -0.0054007 & 5.7634 & 0 & 0 & -9.785 & 0 & 0 \\ 0 & 1.0021 & 0 & -3.8798 \times 10^{-4} & -0.50424 & 0 & 0 & 0 & 0 & 0 \\ 0.027569 & 0 & -0.99552 & 0 & 0 & -0.099411 & 0.042187 & 0 & 0 & 0 \\ 1 & 0 & 0.027603 & 0 & 0 & 0 & 0 & 0 & 0 & 0 \\ 0 & 1 & 0 & 0 & 0 & 0 & 0 & 0 & 0 & 0 \\ 0 & 0 & 1 & 0 & 0 & 0 & 0 & 0 & 0 & 0 \\ 0 & 0 & 0 & 0 & -232.49 & 0 & 0 & 232.49 & 0 & 0 \end{pmatrix}_{10 \times 10} \quad (\text{B.2})$$

$$B_0 = \begin{pmatrix} 0.0 & 0.23 & 0.060 & 0.0 & 0.000000053 & 0.000000030 & -0.000000030 & -0.000000053 \\ 2.3 & -1.7 \times 10^{-13} & -1.2 \times 10^{-13} & 4.3 & 0.000000021 & 0.000000056 & 0.000000056 & 0.000000021 \\ 0.0 & 0.014 & -0.22 & 0.0 & 0.000000031 & 0.000000018 & -0.000000018 & -0.000000031 \\ 0.0 & 0.0 & 5.5 \times 10^{-13} & 0.0 & 0.000000033 & 0.000000033 & 0.000000033 & 0.000000033 \\ 0.046 & 0.0 & 0.0 & 0.090 & -0.000000010 & -0.000000010 & -0.000000010 & -0.000000010 \\ 0.0 & 0.0 & 0.0036 & 0.0 & 0.0000000050 & 0.0000000050 & -0.0000000050 & -0.0000000050 \\ 0.0 & 0.0 & 0.0 & 0.0 & 0.0 & 0.0 & 0.0 & 0.0 \\ 0.0 & 0.0 & 0.0 & 0.0 & 0.0 & 0.0 & 0.0 & 0.0 \\ 0.0 & 0.0 & 0.0 & 0.0 & 0.0 & 0.0 & 0.0 & 0.0 \\ 0.0 & 0.0 & 0.0 & 0.0 & 0.0 & 0.0 & 0.0 & 0.0 \end{pmatrix}_{10 \times 8} \quad (\text{B.3})$$

$$E_1 = \begin{bmatrix} 0.035849 & 0.0 & 0.0 & 0.0 & 0.0 & 0.0 & 0.0 & 0.0 & 0.0 & 0.0 \\ 0.0 & 0.0 & 0.0025597 & 0.0 & 0.0 & 0.0 & 0.0 & 0.0 & 0.0 & 0.0 \\ 0.0 & 0.0 & 0.0 & 0.0 & 0.0 & 0.010370 & 0.0 & 0.0 & 0.0 & 0.0 \\ 0.0 & 0.053794 & 0.0 & 0.0 & 0.0 & 0.0 & 0.0 & 0.0 & 0.0 & 0.0 \\ 0.0 & 0.0 & 0.0 & 0.0031340 & 0.0 & 0.0 & 0.0 & 0.0 & 0.0 & 0.0 \\ 0.0 & 0.0 & 0.0 & 0.0 & 0.00018055 & 0.0 & 0.0 & 0.0 & 0.0 & 0.0 \\ 0.0091904 & 0.0 & 0.0 & 0.0 & 0.0 & 0.0 & 0.0 & 0.0 & 0.0 & 0.0 \\ 0.0 & 0.0 & 0.0042890 & 0.0 & 0.0 & 0.0 & 0.0 & 0.0 & 0.0 & 0.0 \\ 0.0 & 0.0 & 0.0 & 0.0 & 0.0 & 0.00029875 & 0.0 & 0.0 & 0.0 & 0.0 \\ 0.0 & 0.0 & 0.0 & 0.0 & 0.0 & 0.0 & 0.010035 & 0.0 & 0.0 & 0.0 \\ 0.0 & 0.0 & 0.0 & 0.0 & 0.0 & 0.0 & 0.0 & 0.0 & 0.00027689 & 0.0 \\ 0.0 & 0.00051117 & 0.0 & 0.0 & 0.0 & 0.0 & 0.0 & 0.0 & 0.0 & 0.0 \\ 0.0 & 0.0 & 0.0 & 0.00012457 & 0.0 & 0.0 & 0.0 & 0.0 & 0.0 & 0.0 \\ 0.0 & 0.0 & 0.0 & 0.0 & 0.000033050 & 0.0 & 0.0 & 0.0 & 0.0 & 0.0 \\ 0.0 & 0.056658 & 0.0 & 0.0 & 0.0 & 0.0 & 0.0 & 0.0 & 0.0 & 0.0 \\ 0.0 & 0.0 & 0.0 & 0.31514 & 0.0 & 0.0 & 0.0 & 0.0 & 0.0 & 0.0 \\ 0.0 & 0.0 & 0.0 & 0.0 & 0.016315 & 0.0 & 0.0 & 0.0 & 0.0 & 0.0 \\ 0.0 & 0.0 & 0.0 & 0.0 & 0.0 & 0.0 & 0.0 & 0.0 & 0.0 & 12.359 \\ 0.32916 & 0.0 & 0.0 & 0.0 & 0.0 & 0.0 & 0.0 & 0.0 & 0.0 & 0.0 \\ 0.0 & 0.0 & 0.18005 & 0.0 & 0.0 & 0.0 & 0.0 & 0.0 & 0.0 & 0.0 \\ 0.0 & 0.0 & 0.0 & 0.0 & 0.0 & 0.0030652 & 0.0 & 0.0 & 0.0 & 0.0 \\ 0.0 & 0.0 & 0.00019420 & 0.0 & 0.0 & 0.0 & 0.0 & 0.0 & 0.0 & 0.0 \\ 0.0 & 0.0 & 0.0 & 0.0 & 0.0 & 0.0022309 & 0.0 & 0.0 & 0.0 & 0.0 \\ 0.0 & 0.0 & 0.0 & 7.1054 \times 10^{-15} & 0.0 & 0.0 & 0.0 & 0.0 & 0.0 & 0.0 \\ 0.0 & 0.0 & 0.0 & 0.0 & 0.0 & 0.0 & 0.0 & 0.0 & 0.0 & 12.359 \end{bmatrix}^T \quad (B.4)$$

$$E_2 = \begin{bmatrix} 0.0 & 0.0 & 0.020553 & 0.0 & 0.010875 & 0.0 & 0.0 & 0.0 & 0.0 \\ 0.11524 & 0.0 & 0.0 & 0.0 & 0.0 & 0.0 & 0.0 & 0.50976 & 0.0 \\ 0.0 & 0.0 & 0.0 & 0.0022382 & 0.0 & 0.0068932 & 0.0 & 0.0 & 0.0 \\ 0.0 & 0.0 & 0.0 & 0.0 & 0.0 & 0.0 & 0.0 & 0.0 & 0.0 \\ 0.0 & 0.00038610 & 0.0 & 0.0 & 0.0 & 0.0 & 0.0 & 0.0 & 0.0060085 \\ 0.0 & 0.0 & 0.0 & 0.0 & 0.0 & 0.0 & 0.00067334 & 0.0 & 0.0 \\ 0.0 & 0.0 & 0.0 & 0.0 & 0.0 & 0.0 & 0.0 & 0.0 & 0.0 \\ 0.0 & 0.0 & 0.0 & 0.0 & 0.0 & 0.0 & 0.0 & 0.0 & 0.0 \\ 0.0 & 0.0 & 0.0 & 0.0 & 0.0 & 0.0 & 0.0 & 0.0 & 0.0 \\ 0.0 & 0.0 & 0.0 & 0.0 & 0.0 & 0.0 & 0.0 & 0.0 & 0.0 \end{bmatrix}_{10 \times 9} \quad (B.5)$$

$$F_1 = \begin{bmatrix} 1.0 & 0.0 & 0.0 & 0.0 & 0.0 & 0.0 & 0.0 & 0.0 & 0.0 & 0.0 \\ 1.0 & 0.0 & 0.0 & 0.0 & 0.0 & 0.0 & 0.0 & 0.0 & 0.0 & 0.0 \\ 1.0 & 0.0 & 0.0 & 0.0 & 0.0 & 0.0 & 0.0 & 0.0 & 0.0 & 0.0 \\ 0.0 & 1.0 & 0.0 & 0.0 & 0.0 & 0.0 & 0.0 & 0.0 & 0.0 & 0.0 \\ 0.0 & 1.0 & 0.0 & 0.0 & 0.0 & 0.0 & 0.0 & 0.0 & 0.0 & 0.0 \\ 0.0 & 1.0 & 0.0 & 0.0 & 0.0 & 0.0 & 0.0 & 0.0 & 0.0 & 0.0 \\ 0.0 & 0.0 & 1.0 & 0.0 & 0.0 & 0.0 & 0.0 & 0.0 & 0.0 & 0.0 \\ 0.0 & 0.0 & 1.0 & 0.0 & 0.0 & 0.0 & 0.0 & 0.0 & 0.0 & 0.0 \\ 0.0 & 0.0 & 1.0 & 0.0 & 0.0 & 0.0 & 0.0 & 0.0 & 0.0 & 0.0 \\ 0.0 & 0.0 & 1.0 & 0.0 & 0.0 & 0.0 & 0.0 & 0.0 & 0.0 & 0.0 \\ 0.0 & 0.0 & 0.0 & 1.0 & 0.0 & 0.0 & 0.0 & 0.0 & 0.0 & 0.0 \\ 0.0 & 0.0 & 0.0 & 1.0 & 0.0 & 0.0 & 0.0 & 0.0 & 0.0 & 0.0 \\ 0.0 & 0.0 & 0.0 & 0.0 & 1.0 & 0.0 & 0.0 & 0.0 & 0.0 & 0.0 \\ 0.0 & 0.0 & 0.0 & 0.0 & 1.0 & 0.0 & 0.0 & 0.0 & 0.0 & 0.0 \\ 0.0 & 0.0 & 0.0 & 0.0 & 1.0 & 0.0 & 0.0 & 0.0 & 0.0 & 0.0 \\ 0.0 & 0.0 & 0.0 & 0.0 & 0.0 & 1.0 & 0.0 & 0.0 & 0.0 & 0.0 \\ 0.0 & 0.0 & 0.0 & 0.0 & 0.0 & 1.0 & 0.0 & 0.0 & 0.0 & 0.0 \\ 0.0 & 0.0 & 0.0 & 0.0 & 0.0 & 0.0 & 1.0 & 0.0 & 0.0 & 0.0 \\ 0.0 & 0.0 & 0.0 & 0.0 & 0.0 & 0.0 & 0.0 & 1.0 & 0.0 & 0.0 \\ 0.0 & 0.0 & 0.0 & 0.0 & 0.0 & 0.0 & 0.0 & 0.0 & 1.0 & 0.0 \\ 0.0 & 0.0 & 0.0 & 0.0 & 0.0 & 0.0 & 0.0 & 0.0 & 0.0 & 1.0 \end{bmatrix}_{25 \times 10} \quad (\text{B.6})$$

$$F_2 = \begin{bmatrix} 1.0 & 0.0 & 0.0 & 0.0 & 0.0 & 0.0 & 0.0 & 0.0 \\ 1.0 & 0.0 & 0.0 & 0.0 & 0.0 & 0.0 & 0.0 & 0.0 \\ 0.0 & 1.0 & 0.0 & 0.0 & 0.0 & 0.0 & 0.0 & 0.0 \\ 0.0 & 1.0 & 0.0 & 0.0 & 0.0 & 0.0 & 0.0 & 0.0 \\ 0.0 & 0.0 & 1.0 & 0.0 & 0.0 & 0.0 & 0.0 & 0.0 \\ 0.0 & 0.0 & 1.0 & 0.0 & 0.0 & 0.0 & 0.0 & 0.0 \\ 0.0 & 0.0 & 0.0 & 1.0 & 0.0 & 0.0 & 0.0 & 0.0 \\ 0.0 & 0.0 & 0.0 & 1.0 & 0.0 & 0.0 & 0.0 & 0.0 \end{bmatrix}_{9 \times 8} \quad (\text{B.7})$$

In the following, we provide the Matlab code used to design reliable robust controller mentioned in Theorem 5.

```

%Reliable Controller Design

% This program is used to compute a robust stabilizing controller for a
% system with both actuator faults and system uncertainties.
% Theorem 5 in this thesis has the analytical proof.
% This program needs YALMIP and SeDuMi toolboxes installed.

clear
%Menu
fprintf('\n\n')
fprintf('Actuator Considered for Design\n\n')
fprintf('  1. Elevator\n')
fprintf('  2. Aileron\n')
fprintf('  3.Rudder\n')
fprintf('  4. Stabilizer\n')
fprintf('  0. stop\n')
Acc=input(' Specify Actuator : ');
fp=input('Enter the worst case fault percentage [0-100]: ');
load datamatrices
%datamatrices.mat has A_0,B_0,E_1,E_2,F_1,F_2 mentioned in the Appendix B
fp=fp/100;

%System variables Assignment
A=A_0; B=B_0; Dt_n1=E_1; Dt_n2=E_2;
Ct_1=F_1; Ct_2=F_2; D2=E_2;
C2=F_2;
Q=eye(10); % Weight matrices
R=eye(8);

% LMI variables declaration
Y = sdpvar(10,10,'symmetric');
F = sdpvar(8,10,'full');
S1= diag(sdpvar(25,1)); % Diagonal uncertainty structure for \Delta_1
S2= diag(sdpvar(9,1)); % Diagonal uncertainty structure for \Delta_2

Bft=B;
Bft(:,Acc)=B(:,Acc)*fp; % Modifying input and input weight matrices
Cft=F_2; Cft(:,Acc)=F_2(:,Acc)*fp; C2f=(Cft-Ct_2)*F;

Con = set(Y>0); % Constraints
Con=Con+set(S1>0);
Con=Con+set(S2>0);

% LMI constraint under No fault case
Con=Con+...
set([A*Y-B*F+Y*A'-(B*F)'+Dt_n1*S1*Dt_n1'+Dt_n2*S2*Dt_n2' Y*Ct_1' (C2*F)' Y*sqrt(Q) F'*sqrt(R);...
Ct_1*Y -S1 zeros(25,9) zeros(25,10) zeros(25,8);C2*F zeros(9,25) -S2 zeros(9,10) zeros(9,8);...
sqrt(Q)*Y zeros(10,25) zeros(10,9) -eye(10) zeros(10,8);...
sqrt(R)*F zeros(8,25) zeros(8,9) zeros(8,10) -eye(8)]<0);

% LMI constraint under worst fault case
Con=Con+...
set([A*Y+(Bft-B)*F+Y*A'+((Bft-B)*F)'+Dt_n1*S1*Dt_n1'+Dt_n2*S2*Dt_n2' Y*Ct_1' C2f' Y*sqrt(Q) F'*sqrt(R);...
Ct_1*Y -S1 zeros(25,9) zeros(25,10) zeros(25,8);...
C2f zeros(9,25) -S2 zeros(9,10) zeros(9,8); sqrt(Q)*Y zeros(10,25) zeros(10,9) -eye(10) zeros(10,8);...
sqrt(R)*F zeros(8,25) zeros(8,9) zeros(8,10) -eye(8)]<0);

sol = solvesdp(Con); % Finding a feasible solution to the LMI

Yopt = double(Y); % Retrieving optimized values

S1max = double(S1);
S2max =double(S2);
Fopt = double(F);
X=inv(Yopt);

K=-Fopt*X; %Reliable Controller

```

```
% Calculating eigen values for all fault cases
for i=1:fp*10
    kk=eye(8); % variable to consider all fault percentages
    kk(3,3)=i*.1;
    e(:,i)=eig((A+Dt_n1*S1max*Ct_1)+((B+Dt_n2*S2max*Ct_2)*(eye(8)-kk))*K);
    % e contains eigen values
end

%Plotting eigen values of the closed loop
for i=1:fp*10
    if i==1
        tempe=e(:,i);
        plot(real(tempe),imag(tempe),'oR')
        hold
    else
        i=i+1;
        end
        tempe=e(:,i);
        plot(real(tempe),imag(tempe),'oR')
end
grid on;
legend('Eigen Values');
```

# Vita

Phalgun Kumar Rachinayani was born on September 10, 1980, in Tirupati, India. He did his high school from Kendriya Vidyalaya, Tirupati, and Ratnam Junior College, Nellore. He received his Bachelor of Technology degree in Electronics and Control Engineering in 2002 from Jawaharlal Nehru Technological University, Hyderabad. He started his graduate study in electrical engineering at Louisiana State University, Baton Rouge, USA, in Fall 2003. His area of concentration for his master's thesis was robust control with emphasis in designing and analyzing fault tolerant control. He will be awarded the degree of Master of Science in Electrical Engineering in August 2006.